Beam dynamics with space-charge

Lecture
Master NPAC (Nuclei, Particles, Astroparticles, Cosmology)

Antoine Chance*
Nicolas Pichoff
CEA, IRFU

November 8, 2023

*Corresponding author: antoine.chance@cea.fr

Foreword

This 8 hours lecture was given from 2002, in French, to students at Orsay University in DEA of *Physique et Technologie des Grands Instruments (PTGI)* and of *Modélisation et Instrumentation en Physique (MIP)* and in Master 2 of *Rayonnement et Énergie (RE), Optique Matière Plasma (OMP)* and finally *Accélérateurs de Particules et Interactions avec la Matière (APIM)*. In 2014, it has been reduced to 3 hours and is proposed, in English, to Master 2 of *Nuclei, Particles, Astroparticles, Cosmology (NPAC)*. This document is the English translation of the French document given to the students. It contains a little more information than what has been delivered to students in only 3 hours, but it is not forbidden (and even encouraged) to students to go further according to their interest to this topic.

Its goal is to introduce consequences on beam dynamics in an accelerator of electromagnetic interactions between its charged particles. It is a natural prolongation of the classical beam dynamics lectures formally presented to the students (where particles are considered independent from each other) and uses some of the notions presented in them: the different types of accelerator's elements, the formalism associated to linear (matrix) and non-linear (Hamiltonian) dynamics and the beam model.

The reason of this lecture is the profusion of high intensity linac projects (in particular protons and ions). It is then strongly oriented to this kind of machine. Nevertheless, the space-charge subject is often the main limitation of performances of all types of accelerators.

Contents

Introduction

In the classical beam dynamics lectures (transverse and longitudinal), the transport of independent particles is considered in a linear forces (using matrix formalism) and in non-linear forces (using Hamiltonian formalism) in which the transport of statistical model of the beam can be computed. The interactions between particles are not considered. These courses are prerequisites to the following lecture.

The goal of this lecture is to show the effect of the electromagnetic interaction between the charged particles in the beam, known as the **space-charge** .

In the **first part**, once the general expressions of the **electromagnetic field** and associated forces are introduced, we give their *analytical expression* in some particular (but pertinent) charge distributions and show how to model the effects of surrounding conductors. Then, we describe the most common *numerical methods* allowing to compute the field associated to more complex charge distributions.

In the **second part**, we observe how the space-charge **force** can be *linearised* allowing an easiest treatment of beam transport with matrix formalism.

In the **third part**, we describe how the intrinsic *non-linearity* of space-charge force can play a big role on the beam dynamics, in particular on the *emittance growth*.

1 Space-charge force calculation

1.1 Summary

Beams are made of charged particles. Charge is a particle's property that makes them interact at long distance. This interaction is carried by electromagnetic fields whose flow is constant. Electromagnetic field is made of 2 electric and magnetic vector components of which the proportions depend on the referential where they are calculated. Their expression is given by Liénard-Wiechert fields (for alone particle) or Maxwell equations (for charge densities). At a given position, the field is the superposition of the contribution of all charges.

The simplest model, applied for stationary distributions or in a beam frame, is the static approximation for which the electric field can be computed from the charge distribution and the magnetic field from the static current (moving charge) distribution. If the beam is made of particles having (almost) the same **reduced momentum** $\beta\gamma$, the force on particles induced by magnetic field is $-\beta^2$ times lower than the one induced by electric field. The resulting total force is $\frac{1}{\gamma^2}$ times the electric force. Charges induced in the surrounding conductor can be computed by image charge model. In static approximation, the field associated to the specific distributions can be found. The field (and force) associated to beam uniform distribution varies linearly with distance to the beam center. When the beam distribution is complex, numerical algorithms have to be used. The most efficient (and popular) is the PIC algorithms in which macroparticles (sampling the beam) are deposited on a spatial mesh where electrostatic field is computed. Computation time and accuracy depend on the number of macroparticles and mesh sizes.

1.2 Electromagnetic field generalities

The beam particles are considered rigid and are represented by their **position** $\mathbf{r}$[m] [1][2], in 3D space and their **momentum** $\mathbf{p}$ [$\mathrm{kg\,m\,s^{-1}}$]. The motion equations give their evolutions

[1] Dimension units are printed in square brackets. Annex 1 gives the classical dimensions of the quantities used in this lecture.

[2] Physical quantities are printed in *italic*. They appear in ***italic-bold*** when they are defined for the first time.

with **time** t [s]:

$$\begin{cases} \dfrac{d\mathbf{p}}{dt} = \mathbf{F}\left(\mathbf{r}, \mathbf{p}\right) \\ \dfrac{d\mathbf{r}}{dt} = \dfrac{\mathbf{p}}{\gamma \dot{m}} \end{cases} \tag{1.1}$$

- m [kg] is the particle **rest mass** ,
- $\mathbf{F}$ [N] is the **force** applied to the particles,
- γ [n.u.][3] is the particle **reduced energy** or Lorentz factor, which can be written as a function of the particle momentum and rest mass:

$$\gamma = \sqrt{1 + \left(\frac{\|\mathbf{p}\| \cdot c}{m \cdot c^2}\right)^2} \tag{1.2}$$

- $c = 299\,792\,458\,\mathrm{m\,s^{-1}}$ is the physical constant giving the velocity of a no-mass particle in vacuum (light).

The force acting on particle of charge q [C] and velocity $\mathbf{v}$ [$\mathrm{m\,s^{-1}}$] in an electromagnetic field $(\mathbf{E}, \mathbf{B})$[4] ([$\mathrm{V\,m^{-1}}$], [T]) is the **Lorentz force** :

$$\mathbf{F} = q \cdot (\mathbf{E} + \mathbf{v} \times \mathbf{B}) \tag{1.3}$$

This field is produced:

- either by external elements (quadrupole, cavity, Earth magnetic field…),
- or by the beam particles themselves:
  - either directly,
  - or affecting the accelerator environment (vacuum pipe, for example).

There are generally two ways of considering the beam:

☐ It is a set of N charges q and the associated field is the superposition of the fields generated by each particle.

The field at position M and time t generated by a moving charge q in vacuum is given by **Lienard-Wiechert fields** (given in Figure 1.1):

$$\begin{cases} \mathbf{E}(t) = -\dfrac{q}{4\pi\epsilon_0} \left\{ \dfrac{\mathbf{r} - \beta \cdot r}{\gamma^2 \left(r - \mathbf{r} \cdot \beta\right)^3} + \dfrac{\mathbf{r} \times \left[(\mathbf{r} - \beta \cdot r) \times \dot{\beta}\right]}{c \left(r - \mathbf{r} \cdot \beta\right)^3} \right\} \\ \qquad = \mathbf{E_1}(t) + \mathbf{E_2}(t) \\ \mathbf{B}(t) = \dfrac{1}{c} \dfrac{\mathbf{r}}{r} \times \mathbf{E}(t) \\ \qquad = \mathbf{B_1}(t) + \mathbf{B_2}(t) \end{cases} \tag{1.4}$$

[3] n.u. = no unit.

[4] We choose here to interpret electric and magnetic fields as 2 components of an electromagnetic field whose proportions depend on the frame where they are computed.

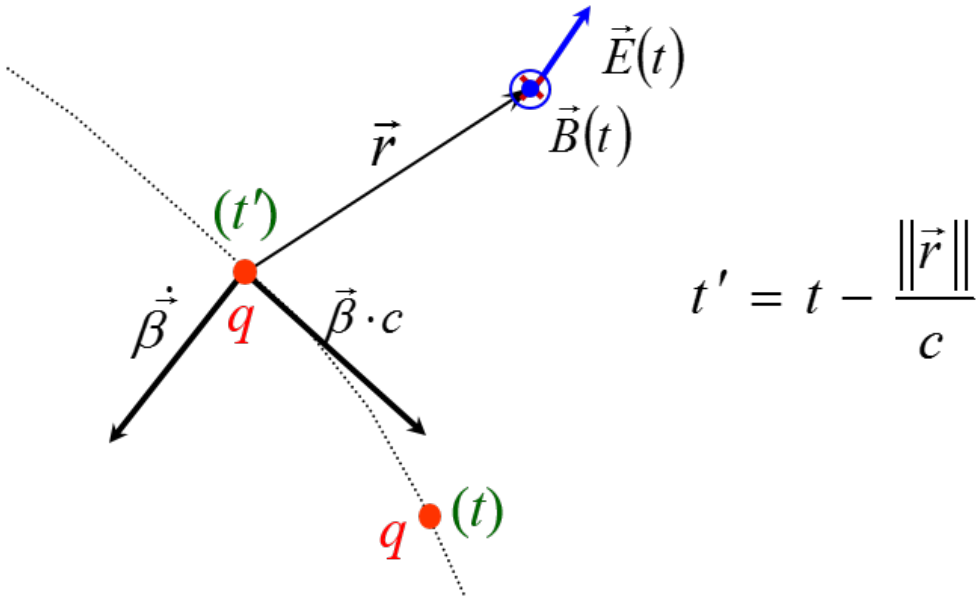

Figure 1.1: Field generated by a moving charge in vacuum.

where:

- $\mathbf{r} = \mathbf{PM}$, P is the particle position at a time t' such as: $\|\mathbf{r}\| = c \cdot (t - t')$,
- $\beta \cdot c$ is the particle velocity at t', β [n.u.] is its **reduced speed** ,
- $\dot{\beta} \cdot c$ is the particle **acceleration** [$\mathrm{m\,s^{-2}}$] at t',
- γ is the particle reduced energy at t'.

The Lienard-Wiechert fields have two components:

- The first, $(\mathbf{E_1}, \mathbf{B_1})$, depends only on the particle position and velocity. This component is well modelled by the electrostatic field in particle frame.
- The second, $(\mathbf{E_2}, \mathbf{B_2})$, depends on the particle acceleration. Every accelerated charged particle radiates an electromagnetic field. Synchrotron radiation (for transverse acceleration) is one example.

☐ It is a **charge density** ρ [$\mathrm{C\,m^{-3}}$] and a **current density** $\mathbf{j}$ [$\mathrm{A\,m^{-2}}$] producing electromagnetic field given by Maxwell equations:

$$\begin{cases} \nabla \cdot \mathbf{E} = \dfrac{\rho}{\epsilon_0} \\ \nabla \times \mathbf{E} = -\dfrac{\partial \mathbf{B}}{\partial t} \\ \nabla \cdot \mathbf{B} = 0 \\ \nabla \times \mathbf{B} = \mu_0 \cdot \mathbf{j} + \dfrac{1}{c^2} \dfrac{\partial \mathbf{E}}{\partial t} \end{cases} \tag{1.5}$$

where:

- $\mu_0 = 4 \times 10^{-7\pi}\,\mathrm{T\,m\,A^{-1}}$ is vacuum magnetic permeability,
- $\epsilon_0 = \frac{1}{\mu_0 \cdot c^2} \approx 8.85 \times 10^{-12}\,\mathrm{C\,V^{-1}\,m^{-1}}$ is the vacuum electric permittivity.

These charge and current densities are either those of the beam (direct space-charge) or those induced by the beam on the surrounding materials (indirect space-charge).

The field is computed with numerical techniques for general charge and current distributions in their specific environment. The solution consists in adding a mesh on the space on which the particles and the field are deposited and their evolutions with time are calculated (see 1.3.4). However, in many cases, the field computation can be simplified using a static model.

1.3 Static model

The space-charge force is calculated in a static approximation in the following cases:

- *When beam is continuous*. Then, one assumes that the charge and current densities are stationary everywhere. Fields are then stationary and electric and magnetic components are independent.
- *In the bunch frame*, where the particle displacements are usually non-relativistic and the field is essentially electrostatic[5]. Once calculated, one can:
  - either apply a Lorentz transform to the fields (with electric and magnetic components, see annex 2) to come back to laboratory frame where the particles dynamics is computed,
  - or compute the particle dynamics in the bunch frame and come back to laboratory frame with Lorentz transform.

The magneto-static field is usually not directly computed from current distribution, but the associated force can often be deduced from the electric one.

1.3.1 Mathematics

☐ A stationary charge density ρ produces an electric field $\mathbf{E}$ solution of:

$$\begin{cases} \nabla \cdot \mathbf{E} = \dfrac{\rho}{\epsilon_0} \\ \nabla \times \mathbf{E} = -\dfrac{\partial \mathbf{B}}{\partial t} \end{cases} \tag{1.6}$$

[5]Be careful to the validity of this assumption for ultra-relativistic beams.

The solution of this system of 2 equations is not direct. It is easier to solve only one scalar equation by noting that: $\nabla \times (\nabla f) = \mathbf{0}$, whatever f function is. One defines the **electrostatic scalar potential** in space ϕ [V][6] such as:

$$\mathbf{E} = -\nabla\phi \tag{1.7}$$

System (1.6) becomes then the **Poisson equation** :

$$\nabla \cdot (\nabla\phi) = \Delta\phi = -\frac{\rho}{\epsilon_0} \tag{1.8}$$

Nevertheless, the beam is not a continuous charge density but is made of charged particles. The electric field $\mathbf{E}$ and the associated potential ϕ produced by a charge q to a distance $\mathbf{r}$ in vacuum are given by:

$$\begin{cases} \mathbf{E} = \dfrac{q}{4\pi\epsilon_0} \dfrac{\mathbf{r}}{\|\mathbf{r}\|^3} \\ \phi = \dfrac{q}{4\pi\epsilon_0} \dfrac{1}{\|\mathbf{r}\|} \end{cases} \tag{1.9}$$

The higher the charge is or the nearer the charge is, the higher the field and potential intensities are.

☐ A stationary current density $\mathbf{j}$ produces a magnetic field $\mathbf{B}$ solution of:

$$\begin{cases} \nabla \cdot \mathbf{B} = 0 \\ \nabla \times \mathbf{B} = \mu_0 \cdot \mathbf{j} \end{cases} \tag{1.10}$$

As for electric field, the solution of a system of 2 equations is not direct. It is easier to solve only one scalar equation by noting that: $\nabla \cdot (\nabla \times \mathbf{f}) = 0$, whatever the vectorial function $\mathbf{f}$ is. One defines the **magnetic vector potential** $\mathbf{A}$, equivalent to electric scalar potential ϕ [7], such as:

$$\mathbf{B} = \nabla \times \mathbf{A} \tag{1.11}$$

System (1.10) becomes then:

$$\nabla \times \nabla \times \mathbf{A} = \mu_0 \cdot \mathbf{j} \tag{1.12}$$

Magnetic field $\mathbf{B}$ and vector potential $\mathbf{A}$ produced by a charge q moving at speed $\mathbf{v}$ to a distance $\mathbf{r}$ in vacuum are given by **Biot-Savart's law** :

$$\begin{cases} \mathbf{B} = \dfrac{\mu_0}{4\pi} \dfrac{q \cdot \mathbf{v} \times \mathbf{r}}{\|\mathbf{r}\|^3} \\ \mathbf{A} = \dfrac{\mu_0}{4\pi} \dfrac{q \cdot \mathbf{v}}{\|\mathbf{r}\|} \end{cases} \tag{1.13}$$

The higher the current (charge and velocity) or the nearer the charge, the higher the field and vector potential intensities are.

[6] Note that, because gradient of a constant is zero, this potential is defined within a constant.

[7] Note that, because curl of a gradient is zero, this vector potential is defined within a gradient of a scalar.

1.3.2 Conductor influence – Image-charge model

When a charge approaches a conductor, charges move in the conductor in order to keep constant the potential (i.e. to cancel the field tangent component) on its surface[8]. With simple geometries, this surface charge distribution can be replaced advantageously by virtual charges, called the **image-charges** , at obvious position. This resulting field is then the same as with the real charges (in the region between the real charges).

Let's have a look on simple configurations: the plate and the cylindrical conductors.

The conducting plate

One can show that if a charge q is placed at a distance d from a conducting plate, the field configuration is well reproduced by putting an image-charge $-q$ at a distance d on the other side of the plate (Figure 1.2). It is easy to show that the electric field tangent component cancels everywhere on the plate surface.

This configuration can be found in electron guns where electrons are emitted from a flat cathode. In that case, the image charge retains (a little) the emitted electrons.

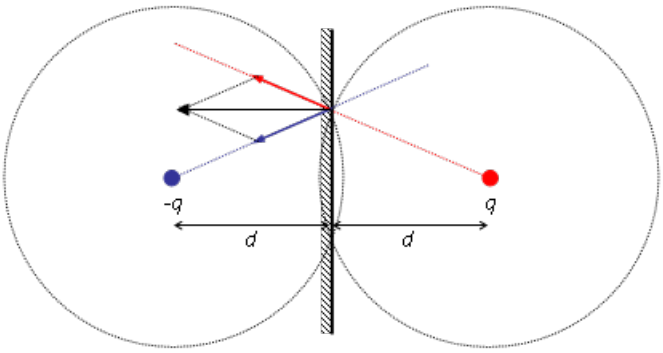

Figure 1.2: Image-charge on a conducting plate.

When the charge travels between two conducting plates (inside a dipole, for example), the induced charge distributions on each plate induces also charges on the other one and so on. This effect can be modelled by an infinite number of image-charges. The real charge first induces 2 image-charges (order 1) on each plate. These image-charges induce image-charges (order 2) on the other plate, and so on. The field is then a superposition of an infinite number of slighter and slighter contributors to field (distance between image-charges and plates increase with the order). This treatment can be found, for example, in CERN courses[9].

[8] If a tangent electric field still exists in the conductor it moves charges until its complete cancellation. The time constant of this phenomenon explains varying behaviour when the field varies rapidly (skin depth, complex impedance...).

[9] From Karlheinz Schindl, Space charge, CERN-2005-004, `http://doc.cern.ch/archive/electronic/cern/preprints/ps/ps-99-012.pdf`.

The conducting cylinder

A cylinder with radius R contains a charge per linear meter λ at a position a from the cylinder axe. The electric field tangent component can be cancelled if the image charge is a charge per linear meter $-\lambda$ on the real charge side, to a distance $b = \frac{R^2}{a}$ from the cylinder axis (Figure 1.3).

One notes that if the charge per linear meter is on cylinder axis, the associated image-charge is ad infinitum.

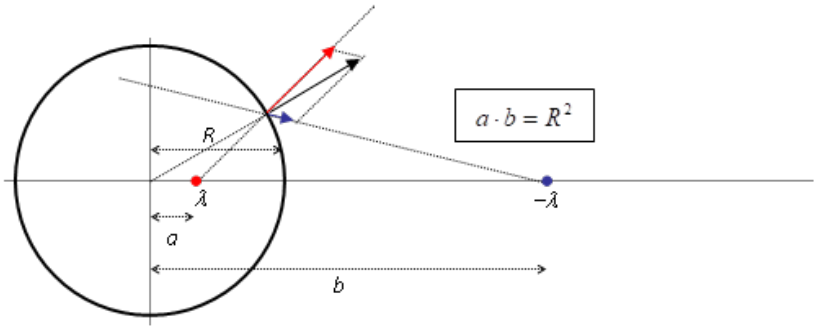

Figure 1.3: Image-charge on a conducting cylinder.

1.3.3 Examples of charge distributions

The electric field configuration associated to some specific charge distributions can be calculated analytically. Here are some examples.

Continuous beam with cylindrically symmetric distributions

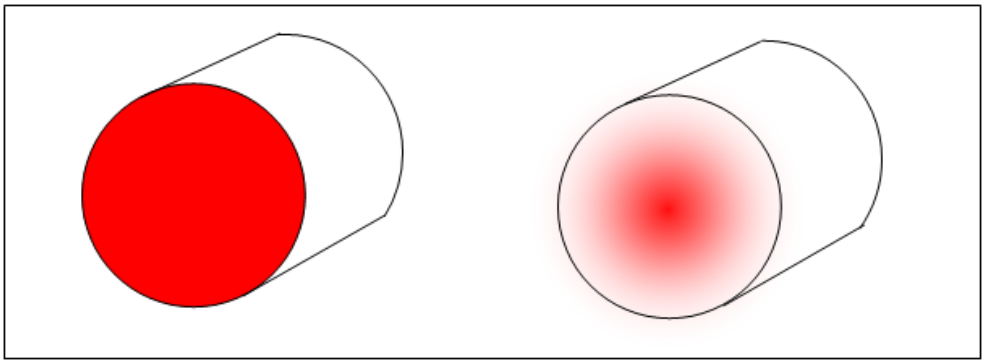

Figure 1.4: Continuous beam with cylindrically symmetric distributions

☐ General charge density of a continuous beam with cylindrically symmetric distributions:

$$\rho\left(x,y,z\right)=\rho\left(r=\sqrt{x^2+y^2}\right) \tag{1.14}$$

Gauss theorem on a cylinder centred on beam axis gives:

$$E_r(r)=\frac{1}{\epsilon_0\cdot r}\int_0^r r'\cdot\rho(r')\cdot dr' \tag{1.15}$$

The current density is:

$$\mathbf{j}\left(x,y,z\right)=j\left(r=\sqrt{x^2+y^2}\right)\cdot\mathbf{u}_z \tag{1.16}$$

$\mathbf{u}_z$ is the unit vector along average beam propagation direction.

If all beam particles have the same longitudinal velocity:

$$\mathbf{v}_z=\bar{\beta}_z c\cdot\mathbf{u}_z \tag{1.17}$$

One has:

$$\mathbf{j}(r)=\rho(r)\cdot\bar{\beta}_z c\cdot\mathbf{u}_z \tag{1.18}$$

Ampere theorem on a cylinder centred on beam axis gives:

$$B_\theta(r)=\frac{\mu_0}{r}\int_0^r r'\cdot\mathbf{j}(r')\cdot dr' \tag{1.19}$$

then:

$$B_\theta(r)=\frac{\mu_0\cdot c}{r}\cdot\bar{\beta}_z\cdot\int_0^r r'\cdot\rho(r')\cdot dr' \tag{1.20}$$

$$\Rightarrow\quad cB_\theta(r)=E_r(r)\cdot\bar{\beta}_z \tag{1.21}$$

The magnetic field is proportional to the electric field.

The impact on the space-charge force is the following. Let's F_r be the radial component of the force acting on a particle of charge q and velocity $\mathbf{v}=v_z\cdot\mathbf{u}_z$:

$$F_r=q\left(E_r-v_z\cdot B_\theta+v_\theta\cdot B_z\right)=q\left(E_r-\beta_z c\cdot B_\theta\right) \tag{1.22}$$

$$\boxed{F_r=q\cdot E_r(r)\cdot\left(1-\beta_z\cdot\bar{\beta}_z\right)} \tag{1.23}$$

The **paraxial approximation** consists in assuming:

$$\beta_2 = \beta_x^2 + \beta_y^2 + \beta_z^2 \approx \beta_z^2 \tag{1.24}$$

with: $\bar{\beta}_z$ independent of r, and: $\left|1 - \frac{\beta_z}{\bar{\beta}_z}\right| \ll 1$ for all beam particles. One gets:

$$\boxed{F_r \approx q \cdot E_r(r) \cdot \left(1 - \beta^2\right) = \frac{q \cdot E_r(r)}{\gamma^2}} \tag{1.25}$$

Remarks:

- At high energy, the magnetic force (largely) compensates the electric one. The space-charge force varies in $\frac{1}{\gamma^2}$. This model always underestimates the space-charge effect as one has always: $\beta_z \cdot \bar{\beta}_z \leq \beta^2$. In some cases (high beam energy, divergence and dispersion) this approximation can lead to big underestimation of space-charge.

☐ If the transverse beam size is negligible, the beam is a "simple" charge per linear meter:

$$\left\{\rho(x, y, z) = \lambda_0 \cdot \delta(r) E_r(r) \quad = \frac{\lambda_0}{2\pi\epsilon_0} \cdot \frac{1}{r} \right. \tag{1.26}$$

Remarks:

- As the field goes down in $\frac{1}{r^2}$ around a particle (flux conservation through a sphere), it goes down in $1/r$ around a charge per linear meter (flux conservation through a cylinder).
- The charge per linear meter λ_0 is linked to the current I_0 through the beam particle average velocity v_0: $I_0 = \lambda_0 \cdot v_0$.
- From the expression of the linear charge per meter, it is possible to compute the electric field associated to all continuous beams by integration over the surface.

☐ Uniform beam distribution (Figure 1.4 - left):

$$\rho(r) = \begin{cases} \rho_{0,h} & \text{if } r < R_h \\ 0 & \text{if } r \geq R_h \end{cases} \tag{1.27}$$

The charge distribution per linear meter is:

$$\lambda = \rho_{0,h} \cdot \pi \cdot R_h^2 \tag{1.28}$$

$$E_r(r) = \begin{cases} \frac{\lambda}{2\pi\epsilon_0} \cdot \frac{r}{R_h^2} & \text{if } r < R_h \\ \frac{\lambda}{2\pi\epsilon_0} \cdot \frac{1}{r} & \text{if } r \geq R_h \end{cases} \tag{1.29}$$

Remarks:

- The field grows linearly with r in the beam.
- Out of the beam, the field is the same as if all the charge per linear meter was placed on its center. It varies in $1/r$.

☐ Parabolic beam distribution:

$$\rho(r) = \begin{cases} \rho_{0,p} \cdot \left(1 - \frac{r^2}{R_p^2}\right) & \text{if } r < R_p \\ 0 & \text{if } r \geq R_p \end{cases} \tag{1.30}$$

The charge distribution per linear meter is:

$$\lambda = \frac{1}{2} \cdot \rho_{0,p} \cdot \pi \cdot R_p^2 \tag{1.31}$$

$$E_r(r) = \begin{cases} \frac{\lambda}{\pi\epsilon_0} \cdot \frac{r}{R_p^2} \cdot \left(1 - \frac{r^2}{2 \cdot R_p^2}\right) & \text{if } r < R_p \\ \frac{\lambda}{2\pi\epsilon_0} \cdot \frac{1}{r} & \text{if } r \geq R_p \end{cases} \tag{1.32}$$

Remarks:

- The field non-linearly varies with r in the beam.
- Out of the beam, the field is the same as if all the charge per linear meter was placed on its center. It varies in $1/r$.

☐ Gaussian beam distribution (Figure 1.4 - right):

$$\rho(r) = \rho_{0,g} \cdot \exp\left(-\frac{r^2}{2 \cdot \sigma_r^2}\right) \tag{1.33}$$

The charge distribution per linear meter is:

$$\lambda = 2 \cdot \rho_{0,g} \cdot \pi \cdot \sigma_r^2 \tag{1.34}$$

$$E_r(r) = \frac{\lambda}{2\pi\epsilon_0} \cdot \frac{1}{r} \cdot \left(1 - \exp\left(-\frac{r^2}{2 \cdot \sigma_r^2}\right)\right) \tag{1.35}$$

Remarks:

- The field varies non-linearly with r in the beam.
- Far from the beam (a few σ_r), the field is the same as if all the charge per linear meter was placed on its center. It varies in $1/r$.

Continuous beam with uniform elliptical distributions

The charge density of a continuous beam with uniform elliptical distributions is:

$$\rho(x,y,z) = \begin{cases} \rho_{0,he} & \text{if } \frac{x^2}{X^2} + \frac{y^2}{Y^2} < 1 \\ 0 & \text{otherwise} \end{cases} \tag{1.36}$$

The charge distribution per linear meter is:

$$\lambda = \rho_{0,he} \cdot \pi \cdot X \cdot Y = \frac{I}{v} \tag{1.37}$$

The electric field at position (x, y) in the beam is the sum of the charges per linear meter over the beam:

$$\begin{cases} E_x(x,y) = \dfrac{\rho_{0,he}}{2\pi \cdot \epsilon_0} \displaystyle\int_{-Y}^{Y} dy' \cdot \int_{-X\sqrt{1-y^2/Y^2}}^{X\sqrt{1-y^2/Y^2}} dx' \frac{x - x'}{\left((x-x')^2 + (y-y')^2\right)^{1/2}} \\ E_y(x,y) = \dfrac{\rho_{0,he}}{2\pi \cdot \epsilon_0} \displaystyle\int_{-X}^{X} dx' \cdot \int_{-Y\sqrt{1-x^2/X^2}}^{Y\sqrt{1-x^2/X^2}} dy' \frac{y - y'}{\left((x-x')^2 + (y-y')^2\right)^{1/2}} \end{cases} \tag{1.38}$$

After integrating:

$$\begin{cases} E_x(x,y) = \dfrac{\lambda}{\pi \cdot \epsilon_0} \cdot \dfrac{1}{X+Y} \cdot \dfrac{x}{X} \\ E_y(x,y) = \dfrac{\lambda}{\pi \cdot \epsilon_0} \cdot \dfrac{1}{X+Y} \cdot \dfrac{y}{Y} \end{cases} \tag{1.39}$$

Remarks:

- The field linearly varies with x and y in the beam.
- Out of the beam, the computation has no analytical solution. However, for $|x| \gg X$ or $|y| \gg Y$, the field varies in $1/r$.

Bunched beam with spherically symmetric distribution

☐ General charge density of a bunched beam with spherically symmetric distributions:

$$\rho\,(x,y,z) = \rho\left(r = \sqrt{x^2+y^2+z^2}\right) \tag{1.40}$$

Gauss theorem on a sphere centred on the beam gives:

$$E_r(r) = \frac{1}{\epsilon_0 \cdot r^2} \int_0^r r'^2 \cdot \rho(r') \cdot dr' \tag{1.41}$$

☐ Uniform beam distribution:

$$\rho(r) = \begin{cases} \rho_{0,h} & \text{if } r < R_h \\ 0 & \text{if } r \geq R_h \end{cases} \tag{1.42}$$

The bunch charge is:

$$Q = \rho_{0,h} \cdot \frac{4\pi}{3} R_h^3 \tag{1.43}$$

$$E_r(r) = \begin{cases} \frac{Q}{4\pi\epsilon_0} \cdot \frac{r}{R_h^3} & \text{if } r < R_h \\ \frac{Q}{4\pi\epsilon_0} \cdot \frac{1}{r^2} & \text{if } r \geq R_h \end{cases} \tag{1.44}$$

Remarks:

- The field linearly varies with r in the beam.
- Out of the beam, the field is the same as if all the beam charge was placed on its center. It varies in $1/r^2$.

☐ Parabolic beam distribution:

$$\rho(r) = \begin{cases} \rho_{0,p} \left(1 - \frac{r^2}{R_p^2}\right) & \text{if } r < R_h \\ 0 & \text{if } r \geq R_h \end{cases} \tag{1.45}$$

The bunch charge is:

$$Q = \frac{2}{5} \rho_{0,p} \cdot \frac{4\pi}{3} R_p^3 \tag{1.46}$$

$$E_r(r) = \begin{cases} \frac{Q}{4\pi\epsilon_0} \cdot \frac{r}{R_p^3} \frac{5}{2} \left(1 - \frac{3}{5} \frac{r^2}{R_p^2}\right) & \text{if } r < R_p \\ \frac{Q}{4\pi\epsilon_0} \frac{1}{r^2} & \text{if } r \geq R_p \end{cases} \tag{1.47}$$

Remarks:

- The field non-linearly varies with r in the beam.
- Out of the beam, the field is the same as if all the charge was placed on its center. It varies in $1/r^2$.

1.3.4 Numerical methods

In usual codes, the beam is represented by N **macroparticles** . Each macroparticle can be considered as a sample of a real particle following the same dynamics (Lorentz equations). Some mathematicians also like considering them as Dirac functions sampling the beam distribution function of which dynamics is given by the Vlasov equation solved (integrated) by a Monte-Carlo method.

Whatever the way to consider it, each macroparticle carries generally a higher charge than the real one (but also a higher mass in order to keep the same ratio q/m, and then the same dynamics). These macroparticles are transported, step by step, through the accelerator structure by computing the applied forces at each time step dt or length step ds solving their motion equations (see Eq. (1.3)). The space-charge force is computed using a space-charge routine. Basis of some of these routines are presented here.

Particle-Particle Interaction (PPI) methods

For each beam macroparticle labelled i, **PPI methods** assume that the space-charge is the sum of the electrostatic fields produced by all other beam particles labelled j:

$$\mathbf{E}_i = \frac{q}{4\pi\epsilon_0} \sum_{j \neq i} \frac{\mathbf{r}_i - \mathbf{r}_j}{\|\mathbf{r}_i - \mathbf{r}_j\|^3} \tag{1.48}$$

Advantages:

- Very easy to encode.
- Direct field on particle is calculated (no mesh needed).

Drawbacks:

- Calculation time T proportional to the square of macroparticle number ($T \propto N^2$),
- Not smooth (high granularity with low N), leading to spurious emittance growth.
- Spurious collisions (due to discrete time step) needing a special treatment for low impact parameter collisions.

Particles In Cells (PIC) methods

The physical space is meshed. The number of mesh cells is n. The mesh dimension can go from 1D to 3D, depending on the problem symmetry. The mesh size is linked either to the beam size or to the accelerator size.

An approximation of the average beam density can be computed in each cell by counting the number of particles inside or close to it (with a possible smoothing effect). The electric field at mesh nodes can be computed from the obtained density using Poisson equation Eq. (1.8). Many techniques can be used to solve this equation:

- Direct methods where the contribution of each lattice is summed over each node. The calculation time is then proportional to the square of the number of mesh cells ($T \propto n^2$).

- FFT methods, noting that the field is the convolution product between the charge density and the Green function G:

$$\phi(x_0, y_0, z_0) = \frac{1}{4\pi\epsilon_0} \iiint_{\text{space}} \frac{\rho(x, y, z)}{\sqrt{(x - x_0)^2 + (y - y_0)^2 + (z - z_0)^2}} dx \cdot dy \cdot dz \tag{1.49}$$

$$= (\rho * G)(x, y, z) \tag{1.50}$$

$$\text{With :} G = \frac{1}{4\pi\epsilon_0} \cdot \frac{1}{\sqrt{x^2 + y^2 + z^2}}. \tag{1.51}$$

  Remarking that the Fourier transform of a convolution product of functions is the product of the Fourier transforms of these functions, one has:

$$\phi(x, y, z) = FFT^{-1}\left(FFT(\rho) \times FFT(G)\right) \tag{1.52}$$

  Calculation time is $T \propto n \log n$. Unfortunately this method does not take into account boundary conditions.

- Relaxation methods, illustrated in 1D as followed. Poisson equation is:

$$\frac{\partial^2 \phi}{\partial x^2} = -\frac{\rho(x)}{\epsilon_0} = \rho'(x) \tag{1.53}$$

  Sampling on the mesh, it becomes:

$$\phi_{i+1} - 2\phi_i + \phi_{i-1} = \rho'_i \cdot \delta^2 \tag{1.54}$$

  i being the cell number, and δ the cell size.

  Relaxation consists in iterating in order to minimize: $|\phi_{i+1} - 2\phi_i + \phi_{i-1} - \rho' i_i \cdot \delta^2|$. At first iteration, $k = 0$, one uses a guessed solution, then, for each k, one computes:

$$\phi_i^{k+1} = \frac{1}{2 + \eta} \left(\phi_{i+1}^k + \phi_{i-1}^k - \rho'_i \cdot \delta^2 + \eta \phi_i^k\right) \tag{1.55}$$

  η is free and generally chosen to accelerate (over-relaxation) or stabilize (under-relaxation) the convergence. It is also possible to use potential already found at $k + 1$.

  The most efficient acceleration is the **multi-grids algorithm** relaxing on many superimposed grids with different cell sizes (for example with 4, 8, 16, 32, 64, 128, 256 cells in each direction). The efficiency of this algorithm is due to the fast transport of rough information from mesh's end to end with a low number of cells (large wavelength) and refinement with high number of lattices (small wavelength). Calculation time is $T \propto n \log n$.

  The relaxation method allows to take into account boundary conditions such as conductors, for example.

PIC methods are the most used, efficient and fast. A good balance between the number of particles and number of mesh cells has to be found. From the one hand, a large number of particles per cell will smooth the distribution function reducing the statistical spurious emittance growth. From the other hand, a bigger cell will also reduce the resolution, hiding precise effects. All methods have not the same sensitivity to the cell size. Some filters can reduce the impact of some phenomena.

Once the field is known at mesh nodes, it is interpolated at particle positions. Many methods with different simplicity, precision or smoothing exist. One part of the space-charge routine calculation time (charge deposition and field calculation) is proportional to the number of macroparticles $T \propto N$.

2 Motion Linearization

2.1 Summary

The particle dynamics is described as a function of an independent variable s which can be time, **curved abscissa** or another variable well matched to the motion.

Each particle is described by 6 coordinates ($\mathbf{P}$, 6D vector) evolving with the independent variable.

- Three coordinates $\mathbf{r}$ represent the particle position in 3D space in an adequate frame (Cartesian, cylindrical ...).
- Three coordinates $\mathbf{p}$ represent the particle motion in 3D space, which is a function of the derivative with s of particle position. It can be velocity, momentum, slope, energy...

The particle dynamics is described by a system giving an expression of the derivative of $\mathbf{P}$ as a function of $\mathbf{P}$ and s:

$$\frac{d\mathbf{P}}{ds} = g(\mathbf{P}, s) \tag{2.1}$$

A force[1] $\mathbf{F}$ can be defined as the derivative of the motion with respect to s:

$$\mathbf{F}(\mathbf{r}, \mathbf{p}, s) = \frac{d\mathbf{p}}{ds} \tag{2.2}$$

Linearising the motion consists in finding a **linear force** modelling the best the force applied to the particle:

$$F_w(\mathbf{r}, \mathbf{p}, s) \xrightarrow[\text{linearisation}]{} \mathbf{k}_w \cdot \mathbf{r} \tag{2.3}$$

with $w = x, y$, or z.

A beam can be modelled by a set of statistical parameters (second order momentum or rms[2]) that can be transported:

- Either with a matrix formalism (inertial or sigma matrix),
- Or by solving second order differential equations (**envelope equations**).

[1] Force is in Newton [N] if $\mathbf{p}$ is the momentum [$\mathrm{kg\,m\,s^{-1}}$] and s is time [s].

[2] rms: root mean square.

The linearised transport is very fast allowing automatic computation to optimize the accelerator. Every beam can be replaced by its equivalent beam with uniform distribution. The linearisation is particularly valid if the beam rms emittance is conserved. To improve the computation, a macroparticle code, taking into account non-linear effects, should be used in complement.

In order to understand the main mechanisms of beam dynamics, it is very convenient to replace the varying focusing accelerator by its equivalent **continuous focusing channel** . In this channel, it is easier to show how the space-charge reduces the particle oscillation frequency. This relative reduction is called the **space-charge tune depression** .

2.2 Beam distribution momentum – the sigma matrix

The beam is made of a large number of particles of which the 6D distribution, $f(\mathbf{P}, s)$, defines it completely. This distribution can be modelled by its momenta.

The zero order momentum, giving the number of particles in the beam, N:

$$N(s) = \int d^6P \cdot f(\mathbf{P}, s) \tag{2.4}$$

The first order momentum, giving the center of gravity vector:

$$\bar{\mathbf{P}}(s) = \int d^6P \cdot f(\mathbf{P}, s) \cdot \mathbf{P} \tag{2.5}$$

$$\bar{P}_i(s) = \int d^6P \cdot f(\mathbf{P}, s) \cdot P_i \tag{2.6}$$

The second order momentum, giving the distribution variance-covariance matrix:

$$[\sigma](s) = \int d^6P \cdot f\left(\mathbf{P} + \bar{\mathbf{P}}(s), s\right) \cdot \mathbf{P} \cdot \mathbf{P}^T \tag{2.7}$$

$$\sigma_{ij} = \int d^6P \cdot f\left(\mathbf{P} + \bar{\mathbf{P}}(s), s\right) \cdot P_i \cdot P_j \tag{2.8}$$

This matrix is known as the **sigma matrix** of the beam.

When it is linear, the particle motion from a position 1 to a position 2 can be computed using the 6×6 transfer matrix $[T_{2\leftarrow 1}]$ (see transverse dynamics lecture):

$$\mathbf{P}_2 = [T_{2\leftarrow 1}] \cdot \mathbf{P}_1 \tag{2.9}$$

The transfer matrix can be used to transport the beam sigma matrix from 1 to 2:

$$[\sigma]_2 = [T_{2\leftarrow 1}] \cdot [\sigma]_1 \cdot [T_{2\leftarrow 1}]^T \tag{2.10}$$

The use of a sigma matrix is the most common and efficient way to estimate the beam transport very quickly and analytically.

The terms $\sqrt{\sigma_{ii}}$, the standard deviations of the distribution function along each direction, are known as the **rms dimensions** of the beam.

The terms $\sigma_{ij} = \sigma_{ji}, i \neq j$ are known as the **rms coupling** of the beam.

The space-charge impulse can also be linearised and modelled by a transfer matrix (see later).

2.3 Reduction to 2D

This 6D motion is often reduced in a lower number of dimensions assuming no correlation between the directions. There is no correlation between two dimensions (let's say i and j) when the transfer and sigma matrix elements:

$$T_{ij} = T_{ji} = 0; \qquad \sigma_{ij} = \sigma_{ji} = 0 \tag{2.11}$$

The 2D formalism (position (coordinate 1, hereafter $x = P_1 - \bar{P}_1$) and motion (coordinate 2, hereafter $x' = P_2 - \bar{P}_2$)) is very common and specific names and notions are associated to this development.

$$\begin{pmatrix} T_{11} & T_{12} & T_{13} & T_{14} & T_{15} & T_{16} \\ T_{21} & T_{22} & T_{23} & T_{24} & T_{25} & T_{26} \\ T_{31} & T_{32} & T_{33} & T_{34} & T_{35} & T_{36} \\ T_{41} & T_{42} & T_{43} & T_{44} & T_{45} & T_{46} \\ T_{51} & T_{52} & T_{53} & T_{54} & T_{55} & T_{56} \\ T_{61} & T_{62} & T_{63} & T_{64} & T_{65} & T_{66} \end{pmatrix} \begin{matrix} \\ \\ \\ \\ \\ \\ \end{matrix} \begin{matrix} \\ =0 \\ \\ \\ \\ \\ \end{matrix} \begin{matrix} \\ \\ \\ \\ \\ =0 \end{matrix} \tag{2.12}$$

The associated extracted 2×2 sigma matrix is:

$$[\sigma] = \begin{pmatrix} \sigma_{11} & \sigma_{12} \\ \sigma_{21} & \sigma_{22} \end{pmatrix} = \begin{pmatrix} \langle x^2 \rangle & \langle x \cdot x' \rangle \\ \langle x \cdot x' \rangle & \langle x'^2 \rangle \end{pmatrix} \tag{2.13}$$

The following term is the beam **rms emittance** along x direction.:

$$\epsilon_x = \sqrt{\det[\sigma]} = \sqrt{\sigma_{11} \cdot \sigma_{12} - \sigma_{12}^2} \tag{2.14}$$

$$= \sqrt{\langle x^2 \rangle \cdot \langle x'^2 \rangle - \langle x \cdot x' \rangle^2} \tag{2.15}$$

The following term is the beam **rms size** along x direction:

$$\tilde{x} = \sqrt{\sigma_{11}} = \sqrt{\langle x^2 \rangle} \tag{2.16}$$

The following terms are the Twiss parameters of the beam along x direction:

$$\begin{cases} \beta_x = \dfrac{\sigma_{11}}{\epsilon_x} = \dfrac{\langle x^2 \rangle}{\epsilon_x} \\ \gamma_x = \dfrac{\sigma_{22}}{\epsilon_x} = \dfrac{\langle x'^2 \rangle}{\epsilon_x} \\ \alpha_x = -\dfrac{\sigma_{12}}{\epsilon_x} = -\dfrac{\langle x \cdot x' \rangle}{\epsilon_x} \end{cases} \tag{2.17}$$

The beam distribution in this 2D (x, x') sub-phase-space can be modelled by an **ellipse** of which the shape is given by:

$$\gamma_x \cdot x^2 + 2\alpha_x \cdot x \cdot x' + \beta_x \cdot x'^2 = n \cdot \epsilon_x \tag{2.18}$$

2.4 Envelope equations

Particle dynamics is given by:

$$\frac{d\mathbf{p}}{dt} = \mathbf{F}\left(\mathbf{r}, \mathbf{p}, t\right) \tag{2.19}$$

Using the curved abscissa s (position on the **reference trajectory**):

$$\frac{d\mathbf{p}}{ds} = \frac{\mathbf{F}\left(\mathbf{r}, \mathbf{p}, s\right)}{\beta_s \cdot c} \tag{2.20}$$

$\beta_s \cdot c = \frac{ds}{dt}$ is the velocity of the particle projection on the reference trajectory.

To describe the particle dynamics, one uses a **moving frame** $(\mathbf{e}_x, \mathbf{e}_y, \mathbf{e}_z)$ centred on the particle projection on the reference trajectory:

$\mathbf{e}_z$ is along the reference trajectory,
$\mathbf{e}_y$ is vertical upright,
$\mathbf{e}_x$ in horizontal plane, toward the left when sitting on the particle.

Locally: $\beta_s = \beta_z$.

In a magnetic field (no energy gain):

$$\frac{d\left(x' \cdot \beta_x\right)}{ds} = \frac{F_x\left(\mathbf{r}, \beta, s\right)}{\gamma\beta_z \cdot mc^2} \tag{2.21}$$

$$\frac{d\left(y' \cdot \beta_y\right)}{ds} = \frac{F_y\left(\mathbf{r}, \beta, s\right)}{\gamma\beta_z \cdot mc^2} \tag{2.22}$$

Let's make some assumptions:

- Assuming a straight line reference trajectory,
- Assuming paraxial approximation: $\beta \approx \beta_z$.

Then[3]:

$$\frac{d\beta_z}{ds} \approx \frac{d\beta}{dz} = 0 \tag{2.23}$$

Motion equations (2.21) and (2.22) become:

$$\frac{dx'}{ds} = \frac{F_x\left(\mathbf{r}, \beta, s\right)}{\gamma\beta^2 \cdot mc^2} = F'_x\left(\mathbf{r}, \beta, s\right) \tag{2.24}$$

$$\frac{dy'}{ds} = \frac{F_y\left(\mathbf{r}, \beta, s\right)}{\gamma\beta^2 \cdot mc^2} = F'_y\left(\mathbf{r}, \beta, s\right) \tag{2.25}$$

Equations along x and y being similar, let's concentrate on x in the following.

[3]On a circular reference trajectory (with radius R), frame evolution gives: $\frac{d\beta_z}{ds} = -\frac{\beta_z}{R} \cdot x'$.

Let's investigate the evolution of the rms size by deriving twice Eq. (2.16) with s:

$$\tilde{x}'' = \frac{\langle x'^2 \rangle + \langle x \cdot x'' \rangle}{\langle x^2 \rangle^{1/2}} - \frac{\langle x \cdot x' \rangle^2}{\langle x^2 \rangle^{3/2}} \tag{2.26}$$

One assumes here that the beam is centred on the reference trajectory: $\langle x \rangle = 0$ and $\langle x' \rangle = 0$. Otherwise, x and x' should be replaced by: $x - \langle x \rangle$ and $x' - \langle x' \rangle$.

Let's multiply Eq. (2.24) by x and averaging over particles:

$$\langle x \cdot x'' \rangle = \langle x \cdot F'_x(\mathbf{r}, \beta, s) \rangle \tag{2.27}$$

Using Eq. (2.26) in Eq. (2.27), one gets:

$$\boxed{\tilde{x}'' - \tilde{K}_x \cdot \tilde{x} - \frac{\tilde{\epsilon}_x^2}{\tilde{x}^3} = 0} \tag{2.28}$$

This equation, giving the evolution with s of rms beam size along x direction, is known as the horizontal envelope equation.

One finds in Eq. (2.28):

- The beam rms horizontal emittance:

$$\tilde{\epsilon}_x = \sqrt{\langle x'^2 \rangle \cdot \langle x^2 \rangle - \langle x \cdot x' \rangle^2} \tag{2.29}$$

- The **linearisation coefficient** of the force.

$$\boxed{\tilde{K}_x = \frac{\langle x \cdot F'_x(\mathbf{r}, \beta, s) \rangle}{\tilde{x}^2}} \tag{2.30}$$

If the force is uncoupled and linear:

$$\langle x \cdot F'_x(\mathbf{r}, \beta, s) \rangle = K_x \cdot x \tag{2.31}$$

One has, from Eq. (2.30): $\tilde{K}_x = K_x$

In 3D, there are 3 envelope equations (one along each direction) coupled through the force. Computing the envelope equations is equivalent to transporting the sigma matrix but is often more complex. However, equations envelopes allow:

- to tell how to linearise the force in Eq. (2.30),
- to show how rms emittance appears naturally in beam transport,
- to gives some analytic solutions of simple case,
- to bring a physical understanding of the beam evolution.

Let's have a look on space-charge force linearisation.

2.5 Space-charge force linearisation

Space charge force is linear only if the beam distribution in real space is uniform. Unfortunately, beams are never uniform and the associated space-charge force is intrinsically non-linear. F. Sacherer showed that:

- In a continuous elliptical symmetric beam, space-charge linearisation coefficients of Eq. (2.30) of **equivalent beams** (see definition later on) are the same whatever their distribution, especially the ones of the equivalent uniform beam.
- In a bunched ellipsoidal symmetric beam, space-charge linearisation coefficients of Eq. (2.30) of equivalent beams are almost[4] the same whatever their distribution, especially the one of the equivalent uniform beam.

Two beams are said equivalent beams, if they have the same:

- current (continuous) or charge (bunched),
- Sigma matrix.

All equivalent beams have the same envelope equations (in the same accelerator) to the limit of a constant rms emittance.

Let's investigate the rms emittance evolution:

$$\begin{aligned}\frac{d\tilde{\epsilon}_x^2}{ds} &= \frac{d\left\langle x'^2\right\rangle}{ds}\cdot\left\langle x^2\right\rangle + \left\langle x'^2\right\rangle\cdot\frac{d\left\langle x^2\right\rangle}{ds} - 2\left\langle x\cdot x'\right\rangle\cdot\frac{d\left\langle x\cdot x'\right\rangle}{ds}\\ &= 2\left\langle x'\cdot x''\right\rangle\cdot\left\langle x^2\right\rangle + 2\left\langle x'^2\right\rangle\cdot\left\langle x\cdot x'\right\rangle - 2\left\langle x\cdot x'\right\rangle\cdot\left(\left\langle x'^2\right\rangle + \left\langle x\cdot x''\right\rangle\right)\\ &= 2\left(\left\langle x'\cdot x''\right\rangle\cdot\left\langle x^2\right\rangle - \left\langle x\cdot x'\right\rangle\cdot\left\langle x\cdot x''\right\rangle\right)\end{aligned} \tag{2.32}$$

$$\begin{aligned}\frac{d\tilde{\epsilon}_x^2}{ds} &= \frac{d\left\langle x'^2\right\rangle}{ds}\cdot\left\langle x^2\right\rangle + \left\langle x'^2\right\rangle\cdot\frac{d\left\langle x^2\right\rangle}{ds} - 2\left\langle x\cdot x'\right\rangle\cdot\frac{d\left\langle x\cdot x'\right\rangle}{ds}\\ &= 2\left\langle x'\cdot x''\right\rangle\cdot\left\langle x^2\right\rangle + 2\left\langle x'^2\right\rangle\cdot\left\langle x\cdot x'\right\rangle - 2\left\langle x\cdot x'\right\rangle\cdot\left(\left\langle x'^2\right\rangle + \left\langle x\cdot x''\right\rangle\right)\\ &= 2\left(\left\langle x'\cdot x''\right\rangle\cdot\left\langle x^2\right\rangle - \left\langle x\cdot x'\right\rangle\cdot\left\langle x\cdot x''\right\rangle\right)\end{aligned} \tag{2.33}$$

When the force is uncoupled and linear: $x'' = k\cdot x$, then :

$$\frac{d\tilde{\epsilon}_x^2}{ds} = 2\cdot k\cdot\left(\left\langle x'\cdot x\right\rangle\cdot\left\langle x^2\right\rangle - \left\langle x\cdot x'\right\rangle\cdot\left\langle x^2\right\rangle\right) = 0 \tag{2.34}$$

the rms emittance is constant.

[4] To a few percents.

Otherwise, assuming: $x'' = k \cdot x + \sum_{i>1} k_i \cdot x^i$:

$$\begin{aligned}\frac{d\tilde{\epsilon}_x^2}{ds} &= 2\left(\left\langle x' \cdot \left(k \cdot x + \sum_{i>1} k_i \cdot x^i\right)\right\rangle \cdot \left\langle x^2\right\rangle - \langle x \cdot x'\rangle \cdot \left\langle x \cdot \left(k \cdot x + \sum_{i>1} k_i \cdot x^i\right)\right\rangle\right) \\ &= 2\left(\left\langle x^2\right\rangle \cdot \sum_{i>1} k_i \left\langle x' \cdot x^i\right\rangle - \langle x \cdot x'\rangle \cdot \sum_{i>1} k_i \left\langle x^{i+1}\right\rangle\right) \\ &\neq 0\end{aligned} \tag{2.35}$$

We plotted in Figure 2.1 the transverse density (left) and associated electric field radial component of 4 equivalent continuous cylindrical symmetric beams. Beams with decreasing density are generally denser in the center but with a bigger size than their equivalent uniform beam.

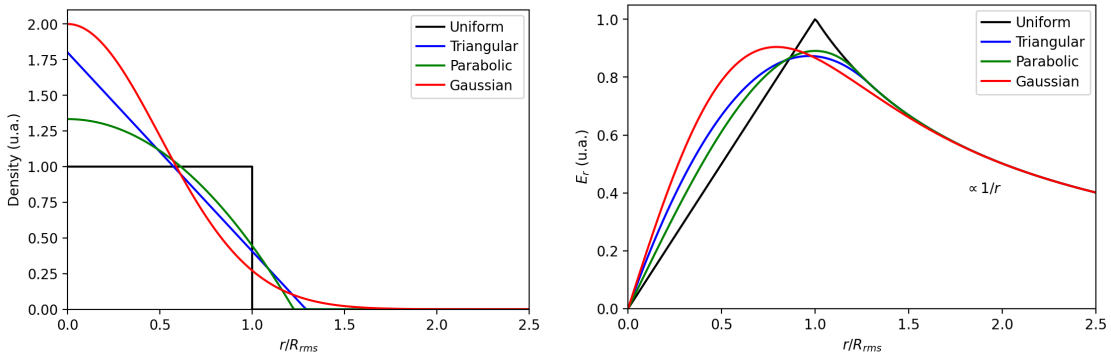

Figure 2.1: Equivalent continuous beams with cylindrical symmetric distributions. Left-radial density; Right-radial electric field.

To linearise the space-charge force of a beam, whatever its distribution, one simply has to:

- compute its rms sizes,
- find its equivalent uniform beam,
- use its linear space-charge force.

Let's investigate the characteristics of continuous and bunched beams with uniform distributions.

2.5.1 Uniform continuous beam

Let's consider a uniform beam with density given by:

$$\rho(x,y) = \begin{cases} \rho_0 & \text{if } \frac{x^2}{X^2} + \frac{y^2}{Y^2} < 1 \\ 0 & \text{otherwise} \end{cases} \tag{2.36}$$

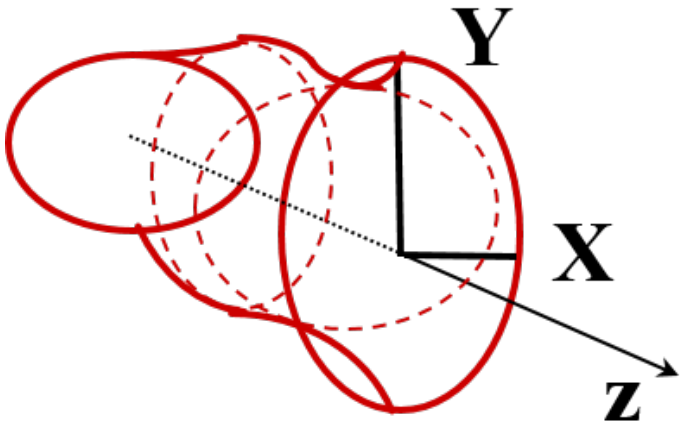

Figure 2.2: Continuous beam with elliptical uniform distribution

X and Y are the beam full sizes.

Rms beam sizes are:

$$\tilde{x} = \frac{X}{2} \qquad\qquad \tilde{y} = \frac{Y}{2} \tag{2.37}$$

If v is the average particle velocity and I the beam current, then:

$$\rho_0 = \frac{I}{\pi \cdot X \cdot Y \cdot v} \tag{2.38}$$

Equation (2.30) gives:

$$\begin{cases} \tilde{K}_{\mathrm{SC},x} = \dfrac{q \cdot I}{2\pi\epsilon_0 m \left(\gamma\beta c\right)^3} \cdot \dfrac{2}{X \cdot (X+Y)} = \dfrac{2 \cdot K}{X \cdot (X+Y)} = \dfrac{K}{2 \cdot \tilde{x} \cdot (\tilde{x}+\tilde{y})} \\ \tilde{K}_{\mathrm{SC},y} = \dfrac{q \cdot I}{2\pi\epsilon_0 m \left(\gamma\beta c\right)^3} \cdot \dfrac{2}{Y \cdot (X+Y)} = \dfrac{2 \cdot K}{Y \cdot (X+Y)} = \dfrac{K}{2 \cdot \tilde{y} \cdot (\tilde{x}+\tilde{y})} \end{cases} \tag{2.39}$$

with the beam **generalized perveance** :

$$K = \frac{q \cdot I}{2\pi\epsilon_0 m \left(\gamma\beta c\right)^3} \tag{2.40}$$

As seen before, the space-charge force of all continuous beams can be linearised using its equivalent uniform beam.

In an uncoupled, linear focusing channel where external force is given by:

$$x'' = -k_{x,0}^2(s) \cdot x \tag{2.41}$$

$$y'' = -k_{y,0}^2(s) \cdot y \tag{2.42}$$

Beam **rms envelope equations** are:

$$\begin{cases} \tilde{x}'' + k_{x,0}^2(s) \cdot \tilde{x} - \dfrac{K/2}{\tilde{x}+\tilde{y}} - \dfrac{\tilde{\epsilon}_x^2}{\tilde{x}^3} = 0 \\ \tilde{y}'' + k_{y,0}^2(s) \cdot \tilde{y} - \dfrac{K/2}{\tilde{x}+\tilde{y}} - \dfrac{\tilde{\epsilon}_y^2}{\tilde{y}^3} = 0 \end{cases} \tag{2.43}$$

The uniform equivalent beam envelope equations are:

$$\begin{cases} X'' + k_{x,0}^2(s) \cdot X - \dfrac{2K}{X+Y} - \dfrac{\epsilon_{x,\text{eff}}^2}{X^3} = 0 \\ Y'' + k_{y,0}^2(s) \cdot Y - \dfrac{2K}{X+Y} - \dfrac{\epsilon_{y,\text{eff}}^2}{Y^3} = 0 \end{cases} \tag{2.44}$$

with:

- the beam **effective emittances** :

$$\epsilon_{x,\text{eff}} = 4 \cdot \tilde{\epsilon}_x \qquad\qquad \epsilon_{y,\text{eff}} = 4 \cdot \tilde{\epsilon}_y \tag{2.45}$$

- the beam **effective sizes** :

$$X = 2 \cdot \tilde{x} \qquad\qquad Y = 2 \cdot \tilde{y} \tag{2.46}$$

2.5.2 Bunched continuous beam

Let's consider a beam with density given by:

$$\rho(x,y) = \begin{cases} \rho_0 & \text{if } \frac{x^2}{X^2} + \frac{y^2}{Y^2} + \frac{z^2}{Z^2} < 1 \\ 0 & \text{otherwise} \end{cases} \tag{2.47}$$

X, Y, and Z are the beam full sizes.

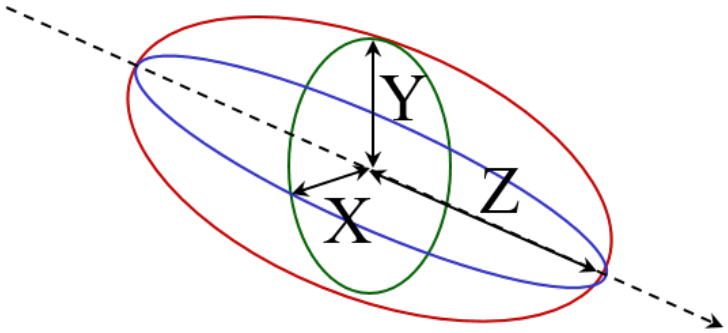

Figure 2.3: Bunched beam with ellipsoidal uniform distribution

Rms beam sizes are:

$$\tilde{x} = \frac{X}{\sqrt{5}} \qquad \tilde{y} = \frac{Y}{\sqrt{5}} \qquad \tilde{z} = \frac{Z}{\sqrt{5}} \tag{2.48}$$

If Q is the bunch charge:

$$\rho_0 = \frac{Q}{\frac{4}{3}\pi \cdot X \cdot Y \cdot Z} \tag{2.49}$$

One has:

$$\begin{cases} \tilde{K}_{\mathrm{SC},x} = \dfrac{q}{mc^2} \cdot \dfrac{3}{4\pi\epsilon_0} \cdot \dfrac{Q}{\beta^2\gamma^2} \cdot \displaystyle\int_0^\infty \dfrac{dt}{\left[(X^2+t)^3 \cdot (Y^2+t) \cdot ((\gamma Z)^2+t)\right]^{1/2}} \\ \tilde{K}_{\mathrm{SC},y} = \dfrac{q}{mc^2} \cdot \dfrac{3}{4\pi\epsilon_0} \cdot \dfrac{Q}{\beta^2\gamma^2} \cdot \displaystyle\int_0^\infty \dfrac{dt}{\left[(X^2+t) \cdot (Y^2+t)^3 \cdot ((\gamma Z)^2+t)\right]^{1/2}} \\ \tilde{K}_{\mathrm{SC},z} = \dfrac{q}{mc^2} \cdot \dfrac{3}{4\pi\epsilon_0} \cdot \dfrac{Q}{\beta^2\gamma^2} \cdot \displaystyle\int_0^\infty \dfrac{dt}{\left[(X^2+t) \cdot (Y^2+t) \cdot ((\gamma Z)^2+t)^3\right]^{1/2}} \end{cases} \tag{2.50}$$

As seen before, the space-charge force of all bunched beams can be linearised using its equivalent uniform beam.

In an uncoupled, linear focusing channel where external force is given by:

$$\begin{cases} x'' = -k_{x,0}^2(s) \cdot x \\ y'' = -k_{y,0}^2(s) \cdot y \\ z'' = -k_{z,0}^2(s) \cdot z \end{cases} \tag{2.51}$$

Beam rms envelope equations are:

$$\begin{cases} \tilde{x}'' + k_{x,0}^2(s) \cdot \tilde{x} - \tilde{K}_{\mathrm{SC},x} \cdot \tilde{x} - \dfrac{\tilde{\epsilon}_x^2}{\tilde{x}^3} = 0 \\ \tilde{y}'' + k_{y,0}^2(s) \cdot \tilde{y} - \tilde{K}_{\mathrm{SC},y} \cdot \tilde{y} - \dfrac{\tilde{\epsilon}_y^2}{\tilde{y}^3} = 0 \\ \tilde{z}'' + k_{z,0}^2(s) \cdot \tilde{z} - \tilde{K}_{\mathrm{SC},z} \cdot \tilde{z} - \dfrac{\tilde{\epsilon}_z^2}{\tilde{z}^3} = 0 \end{cases} \tag{2.52}$$

The uniform equivalent beam envelop equations are:

$$\begin{cases} X'' + k_{x,0}^2(s) \cdot X - \tilde{K}_{\mathrm{SC},x} \cdot X - \dfrac{\epsilon_{x,\mathrm{eff}}^2}{X^3} = 0 \\ Y'' + k_{y,0}^2(s) \cdot Y - \tilde{K}_{\mathrm{SC},y} \cdot Y - \dfrac{\epsilon_{y,\mathrm{eff}}^2}{Y^3} = 0 \\ Z'' + k_{z,0}^2(s) \cdot Z - \tilde{K}_{\mathrm{SC},z} \cdot Z - \dfrac{\epsilon_{z,\mathrm{eff}}^2}{Z^3} = 0 \end{cases} \tag{2.53}$$

with:

- the beam effective emittances:

$$\epsilon_{x,\text{eff}} = 5 \cdot \tilde{\epsilon}_x \qquad \epsilon_{y,\text{eff}} = 5 \cdot \tilde{\epsilon}_y \qquad \epsilon_{z,\text{eff}} = 5 \cdot \tilde{\epsilon}_z \tag{2.54}$$

- the beam effective sizes:

$$X = \sqrt{5} \cdot \tilde{x} \qquad Y = \sqrt{5} \cdot \tilde{y} \qquad Z = \sqrt{5} \cdot \tilde{z} \tag{2.55}$$

Unfortunately, there are no analytical solutions for integrals (2.50). However, when the beam has a cylindrical symmetry around z axis ($X = Y = R$), analytical solutions can be found to equations:

$$\begin{cases} \tilde{K}_{\text{SC},x} = \tilde{K}_{\text{SC},y} = \dfrac{q}{mc^2} \cdot \dfrac{3}{4\pi\epsilon_0} \cdot \dfrac{Q}{\beta^2\gamma^2} \cdot \displaystyle\int_0^\infty \dfrac{dt}{\left(R^2+t\right)^2 \cdot \left((\gamma Z)^2+t\right)^{1/2}} \\ \tilde{K}_{\text{SC},z} = \dfrac{q}{mc^2} \cdot \dfrac{3}{4\pi\epsilon_0} \cdot \dfrac{Q}{\beta^2\gamma^2} \cdot \displaystyle\int_0^\infty \dfrac{dt}{\left(R^2+t\right) \cdot \left((\gamma Z)^2+t\right)^{3/2}} \end{cases} \tag{2.56}$$

2.6 Space-charge tune depression

A **periodic transport channel** with **phase-advance** σ_0 and **period** L can be modelled by a continuous focusing channel applying a continuous force to the beam [see longitudinal beam dynamics lecture][5].

If the force is linear, the particle motion equation in the channel is simply the one of a harmonic oscillator:

$$\frac{d^2x}{ds^2} = -\left(\frac{\sigma_{x,0}}{L}\right)^2 \cdot x = -k_{x,0}^2 \cdot x \tag{2.57}$$

$k_{x,0} = \frac{\sigma_{x,0}}{L}$ is the focusing channel **phase advance per meter** ,

The solution is:

$$x(s) = x_0 \cdot \cos\left(k_{x,0} \cdot s + \varphi\right) \tag{2.58}$$

When linearised space-charge force is added, the focusing force is reduced:

$$\frac{d^2x}{ds^2} = -\left(k_{x,0}^2 - \tilde{K}_{\text{SC},x}\right) \cdot x = -\tilde{k}_x^2 \cdot x \tag{2.59}$$

with:

- The beam **phase advance per meter with space charge** in the channel:

$$\tilde{k}_x = \sqrt{k_{x,0}^2 - \tilde{K}_{\text{SC},x}} = \tilde{\eta} \cdot k_{x,0} \tag{2.60}$$

[5]This approximation allows to reach analytical solutions to explore the space-charge force effects.

- The beam **rms space-charge tune depression** in the channel:

$$\eta = \frac{\tilde{k}_x}{k_{x,0}} \tag{2.61}$$

  It gives the ratio between the particle oscillation average frequency[6] in the beam (with space-charge) and the one of an alone particle (without space-charge). $\tilde{\eta}$ is used to quantify the space-charge influence and goes from 1 to 0 when increasing space-charge.

To explore further its influence, let's use the horizontal rms envelope equation (2.43) with linearised external and space-charge forces:

$$\tilde{x}'' + \left(k_{x,0}^2(s) - \frac{K/2}{2 \cdot \tilde{x} \cdot (\tilde{x} + \tilde{y})} \right) \cdot \tilde{x} - \frac{\tilde{\epsilon}_x^2}{\tilde{x}^3} = 0 \tag{2.62}$$

Two "pressures" contribute to beam defocusing:

- the emittance pressure (similar to a thermal pressure): $\tilde{x}'' \propto \frac{\tilde{\epsilon}_x^2}{\tilde{x}^3}$
- the space-charge pressure: $\tilde{x}'' \propto \frac{K/2}{2 \cdot \tilde{x} \cdot (\tilde{x} + \tilde{y})} \cdot \tilde{x}$

Assuming a round beam, $\tilde{x} = \tilde{y}$, the matched beam is the beam of which the rms size $\tilde{x}_a$ is constant during the transport:

$$\tilde{x}'' = -\tilde{\eta}_a^2 \cdot k_{x,0}^2 \cdot \tilde{x}_a + \frac{\tilde{\epsilon}_x^2}{\tilde{x}_a^3} = 0 \tag{2.63}$$

giving:

$$\tilde{x}_a = \sqrt{\frac{\tilde{\epsilon}_x}{\tilde{\eta}_a \cdot k_{x,0}}} \tag{2.64}$$

From Eq. (2.62), beam dynamics is:

- **Emittance dominated** if: $K \ll 4\frac{\tilde{\epsilon}_x}{\tilde{x}^2}$
- **Space-charge dominated** if:$K \gg 4\frac{\tilde{\epsilon}_x^2}{\tilde{x}^2}$
- In between, it is **space-charge driven** .

It is interesting to observe that, despite of what could be the intuitive, the smaller the beam, the less it is space-charge driven. Space-charge pressure increases more slowly than emittance pressure when the beam size decreases.

[6] In uniform beam (linear force), all particles oscillate at this frequency. Otherwise, the effect will be seen later.

Let's call $\tilde{\eta}_t$ the transition space-charge tune depression for which emittance and space-charge pressures are the same. From Eq. (2.62):

$$\left(1-\tilde{\eta}_t^2\right)\cdot k_{x,0}^2\cdot\tilde{x}_a=\frac{\tilde{\epsilon}_x^2}{\tilde{x}^3}=\tilde{\eta}_t^2\cdot k_{x,0}^2\cdot\tilde{x}_a \tag{2.65}$$

giving:

$$\left(1-2\cdot\tilde{\eta}_t^2\right)\cdot k_{x,0}^2\cdot\tilde{x}_a=0 \tag{2.66}$$

Then:

$$\tilde{\eta}_t=\frac{1}{\sqrt{2}}\approx 0.707 \tag{2.67}$$

The space-charge is twice[7] the emittance pressure for: $\tilde{\eta}_t\leq\frac{1}{\sqrt{3}}\approx 0.58$. The emittance is twice the space-charge pressure for: $\tilde{\eta}_t\geq\frac{1}{\sqrt{1.5}}\approx 0.82$.

The oscillations of an alone particle and of a particle in a space-charge uniform dominated beam with $\tilde{\eta}_t=0.38$ are plotted in Figure 2.4, in a continuous focusing channel (up) and in an equivalent periodic channel (down).

Even with a strong phase advance per lattice (130°) in the periodic channel, motion periodic channel is well modelled by the equivalent continuous one.

2.7 Space-charge kick matrix

The space-charge linear force can be modelled by a **space-charge kick matrix** representing its effect over a distance ds. This kick can be extracted from Eq. (2.59):

$$\left.\frac{dx'}{ds}\right|_{\mathrm{SC}}=\tilde{K}_{\mathrm{SC},x}\cdot x \tag{2.68}$$

$\tilde{K}_{\mathrm{SC},x}$ being given by Eq. (2.30) for continuous or Eq. (2.50) for bunched beam.

The space-charge is then modelled by a space-charge kick matrix, applied regularly (as often as necessary due to beam distribution change) at the center of each step ds:

$$[T_{\mathrm{SC}}]=\begin{pmatrix}1&0&0&0&0&0\\ \tilde{K}_{\mathrm{SC},x}&1&0&0&0&0\\ 0&0&1&0&0&0\\ 0&0&\tilde{K}_{\mathrm{SC},y}&1&0&0\\ 0&0&0&0&1&0\\ 0&0&0&0&\tilde{K}_{\mathrm{SC},z}&1\end{pmatrix} \tag{2.69}$$

With the coordinate vector:

$$\mathbf{P}=\begin{pmatrix}x&x'&y&y'&z&z'\end{pmatrix}^T \tag{2.70}$$

[7]Subjective definition.

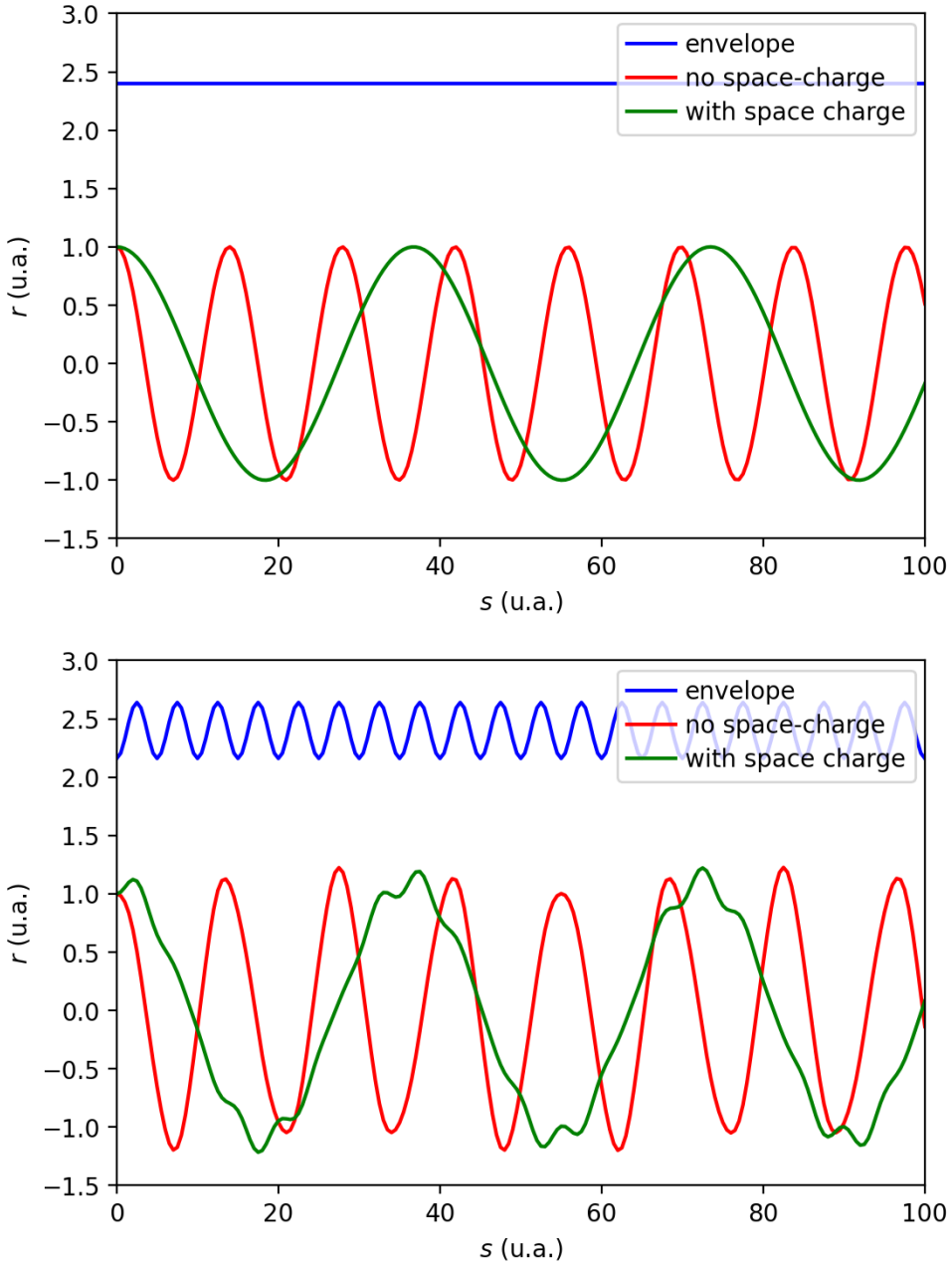

Figure 2.4: Oscillations in a continuous focusing (top) and in an equivalent periodic channel (bottom) of an alone particle (red) and of a particle in a space-charge dominated uniform beam with $\tilde{\eta}_t = 0.38$ (green). The envelope is plotted in blue.

Otherwise, if a different $\mathbf{P}$ is chosen, $\tilde{K}_{\mathrm{SC},w}$ (w for x, y or z) coefficients have to be replaced by adequate functions of $\tilde{K}_{\mathrm{SC},w}$.

Space-charge continuously acts on the beam. In order to compute its effect along the accelerator, each element has to be divided in n sub-elements of length ds at the middle of which the space-charge kick is applied. The beam size has to evolve slowly with respect to ds.

3 Non-linear motion

3.1 Summary

Linearisation is a good tool to evaluate, in a minimal energy and time, its main influence on the beam dynamics and to match the beam in the accelerator. However, space-charge force is intrinsically non-linear and this non-linearity has non-negligible effects to take into account.

With non-linear forces, the oscillation frequency (betatron-transverse and synchrotron-longitudinal) of the particles depends on its oscillation amplitude. With space-charge, the lower the amplitude, the slower the oscillation is. The ratio between frequencies of high and low amplitude particles is the space-charge tune dispersion.

A **perfectly matched** beam, i.e. a beam of which the phase-space distribution stays constant along particle motion in phase-space (on which the motion Hamiltonian is constant), has a stationary distribution with no-emittance growth.

A rms-matched beam is a beam of which sigma matrix is constant (periodic) in a continuous (periodic) focusing channel. It can be realized with linear focusing elements (quadrupoles, solenoids, bunchers). It minimizes the emittance growth.

When a beam is mismatched many phenomena contribute to emittance growth:

- Charge redistribution until perfect matching,
- **Filamentation** until perfect matching,
- Parametric resonant interactions with intrinsic motion of particles and space-charge force oscillation, in particular resonance of order 2 with beam mismatch modes.

3.2 Space-charge tune dispersion

When the beam distribution is non-uniform (almost always) space-charge force is non-linear. As seen in longitudinal motion, in a confining non-linear force, particle oscillation frequency depends on its amplitude.

Let's come back to horizontal motion (equation (2.24)):

$$\frac{dx'}{ds} = F'_x\left(\mathbf{r}, \beta, s\right) \tag{3.1}$$

Assuming continuous, focusing, linear external forces, this becomes:

$$\frac{dx'}{ds} = -k_{x,0}^2 \cdot x + F'_{x,\mathrm{SC}}(\mathbf{r}, s) \tag{3.2}$$

Assuming a space-charge force x component depending only on x (no coupling[1]), force can be written[2]

$$F'_{x,\mathrm{SC}}(\mathbf{r}, s) = \sum_{i>0} k_{x,\mathrm{SC},i} \cdot x^i \tag{3.3}$$

Equation (3.2) becomes:

$$\frac{dx'}{ds} = -\left(k_{x,0}^2 - k_{x,\mathrm{SC},1}\right) \cdot x - \sum_{i>1} k_{x,\mathrm{SC},i} \cdot x^i \tag{3.4}$$

- At low amplitude $\hat{x}$ ($\hat{x}/\tilde{x} \ll 1$), the phase advance per unit length is:

$$\lim_{\hat{x}\to 0} k_x = \sqrt{k_{x,0}^2 - k_{x,\mathrm{SC},1}} = \eta_{x,c} \cdot k_{x,0} \tag{3.5}$$

  with the beam core space-charge tune depression (for small amplitudes):

$$\eta_{x,c} = \sqrt{1 - \frac{k_{x,\mathrm{SC},1}}{k_{x,0}^2}} \tag{3.6}$$

- At very large amplitude ($\hat{x}/\tilde{x} \gg 1$), the particle is mainly out of the beam where the external focusing (proportional to x) is much higher than the space-charge force (in $1/x^k$), the phase advance per unit length tends to:

$$\lim_{\hat{x}\to\infty} k_x = k_{x,0} \tag{3.7}$$

If the beam radial density is decreasing (which is usually the case), the phase advance per unit length k_x is a growing[3] function of the amplitude $\hat{x}$ such as:

$$\eta_{x,c} \cdot k_{x,0} \leq k_x(\hat{x}) < k_{x,0} \tag{3.8}$$

This phenomenon, illustrated in Figure 3.1, is the space-charge tune dispersion.

Note that $\eta_{x,c} \leq \tilde{\eta}_x$ with equality in uniform beam.

[1] The non-coupling is a strong assumption, generally false!.

[2] Note that polynomial development is not very convenient to model forces in $1/x^n$ with large x.

[3] This is valid in all direction (horizontal, vertical and longitudinal). However, the intrinsic non-linear longitudinal force induces phase advance decreasing with the amplitude which can compensate the effect of the space-charge.

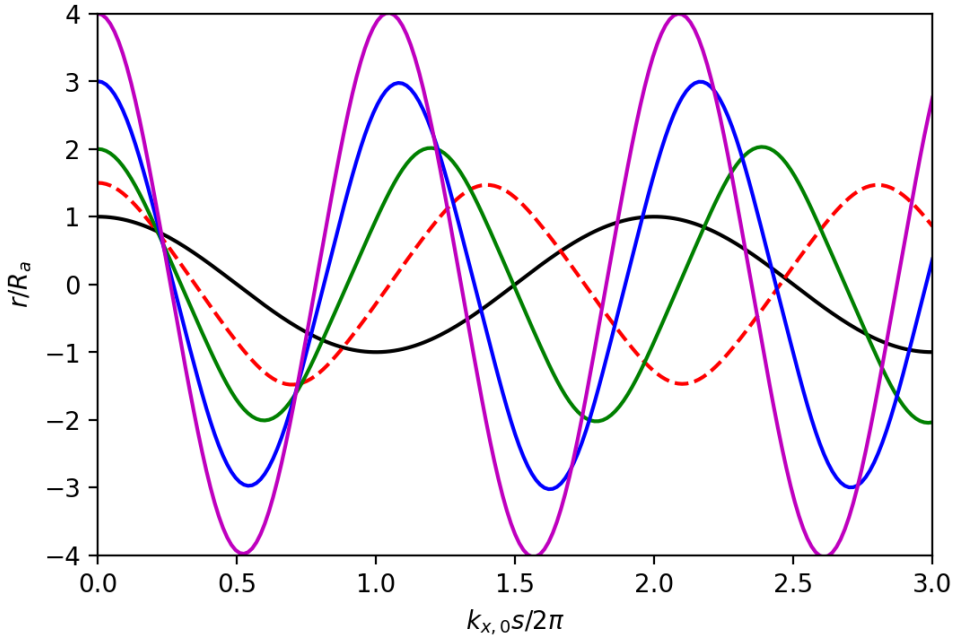

Figure 3.1: Particle oscillations with different amplitudes around a uniform beam with radius R_a.

Let's consider continuous Gaussian beam. The center density is twice higher than in its equivalent uniform beam (Figure 2.1, 27). One has then:

$$\frac{k_{x,\text{SC, Gauss,1}}}{k_{x,0}^2} = 1 - \eta_{x,\text{SC, Gauss}}^2 = \frac{2k_{x,\text{SC, uniform,1}}}{k_{x,0}^2} = 2\left(1 - \tilde{\eta}_x^2\right) \tag{3.9}$$

Giving:

$$\eta_{x,\text{SC, Gauss}} = \sqrt{2\tilde{\eta}_x^2 - 1} \tag{3.10}$$

A Gaussian distribution is unstable if: $\tilde{\eta}_x < \frac{1}{\sqrt{2}}$. In this case, space-charge defocusing force is higher than focusing external force in the beam center. These particles are then increasing their amplitude and the beam distribution changes its shape (and the center density is reduced).

3.3 Perfect matching

Beam matching and mismatching have been presented in transverse and longitudinal beam dynamics. Effects of non-linearity (filamentation) is shown in longitudinal beam dynamics lecture. We introduce here specific effects of space-charge reminding that space-charge is overall a non-linear force.

A beam is perfectly matched to a continuous focusing channel if its phase-space distribution (in 4D for continuous and 6D for bunched beams) is constant over curves on which the particles travel, i.e. on iso-Hamiltonians.

Hamiltonian motion is[4] a function of phase-space coordinates $(\mathbf{r}, \mathbf{p})$ associated to an independent variable t, $H(\mathbf{r}, \mathbf{p}, t)$, such as:

$$\begin{cases} \dfrac{d\mathbf{r}}{dt} = \dfrac{\partial H}{\partial \mathbf{p}} = \nabla_{\mathbf{p}} \cdot H \\ \dfrac{d\mathbf{p}}{dt} = -\dfrac{\partial H}{\partial \mathbf{r}} = -\nabla_{\mathbf{r}} \cdot H \end{cases} \tag{3.11}$$

Equation (3.11) tells that, at each time, particles are moving in phase-space on curves on which the Hamiltonian is constant as shown in Figure 3.2.

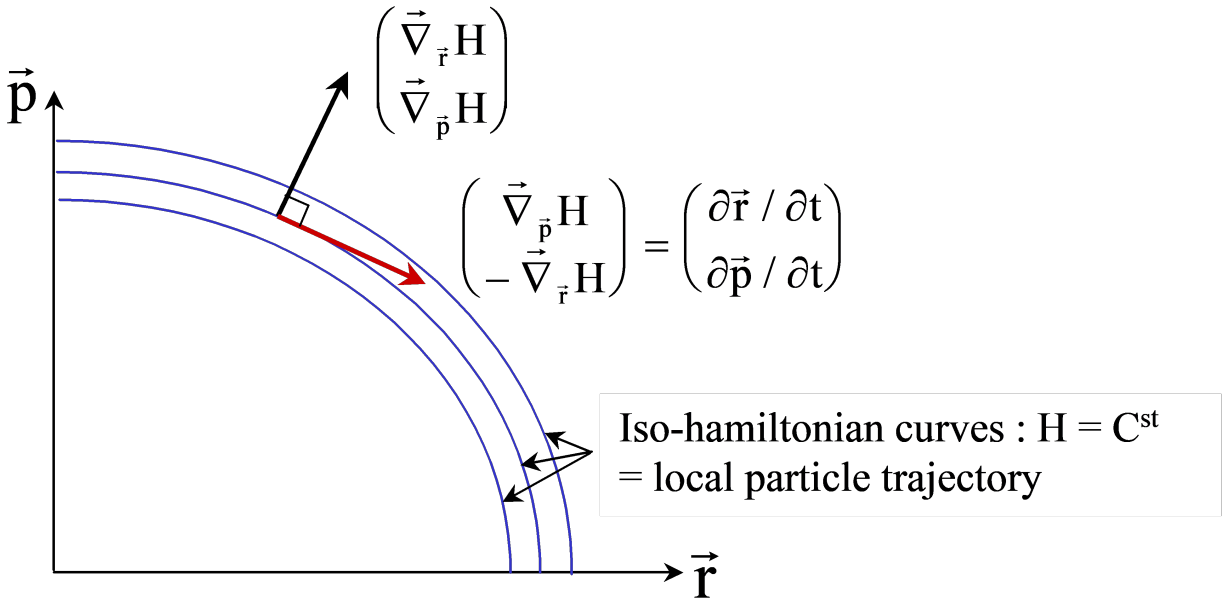

Figure 3.2: Particle motion in phase-space on curves for which the Hamiltonian is constant.

The space-charge specificity, compared to simple external non-linear force, is that the Hamitonian does depend on the particle distribution. A change of particle distribution produces a change in the Hamiltonian, producing a change in the particle trajectories, producing a change in the particle distribution...

A beam is then perfectly matched in a continuous focusing channel if its distribution is stationary, i.e. its distribution through a small particle motion stays the same (or after one period in a periodic channel).

[4]Model presented here is simplified in order to give the right physical intuition in a reasonable time. It is not perfectly true (for example, the canonical conjugate variable to $\mathbf{r}$, $\mathbf{p} + \mathbf{r} \cdot \mathbf{A}$ is replaced here by $\mathbf{p}$), but efficient enough to understand the meaning of what is told. Students who want to go further can look at general mechanics books or CERN courses.

The simplest way to explore stationary distributions is to use the Vlasov equation transporting the beam distribution function f:

$$\frac{\partial f}{\partial t} + \frac{\mathbf{p}}{m} \cdot \nabla_{\mathbf{r}} f + q\left(\mathbf{E} + \frac{\mathbf{p}}{m} \times \mathbf{B}\right) \cdot \nabla_{\mathbf{p}} f = 0 \tag{3.12}$$

where $f(\mathbf{r}, \mathbf{p}, t)$ is the number of particles at time t and at position $(\mathbf{r}, \mathbf{p})$ in a phase-space sub-hyper-volume $d\mathbf{r} \times d\mathbf{p}$.

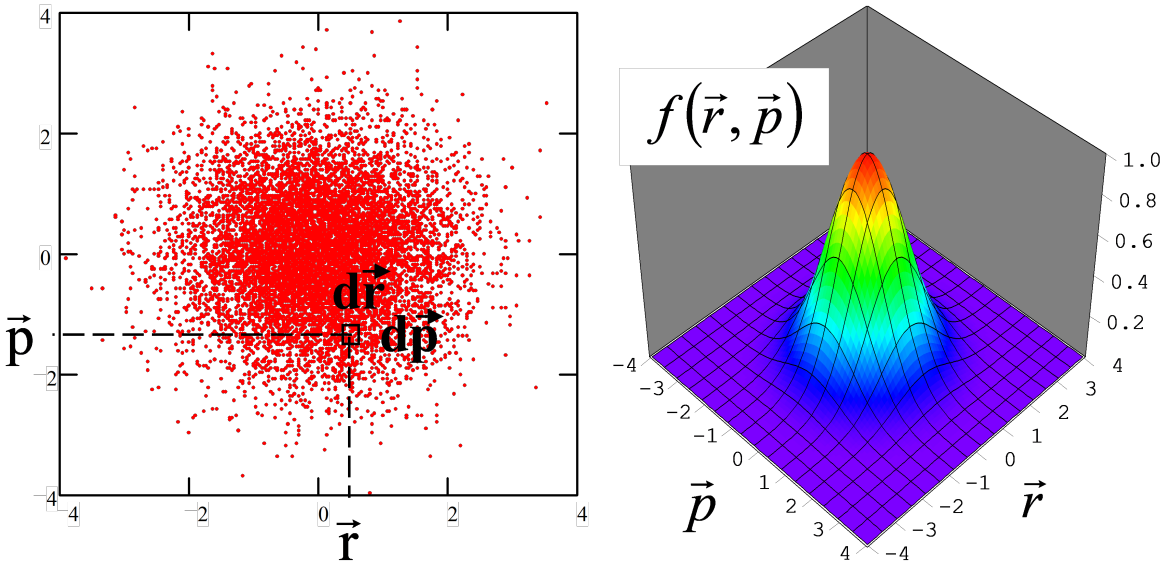

Figure 3.3: Left: particle distribution; right: distribution function.

Distribution function is stationary if $\frac{\partial f}{\partial t} = 0$. It can be proven that this is possible only if the distribution function is constant on curves on which the Hamiltonian is constant:

$$f(\mathbf{r}, \mathbf{p}) = f(H(\mathbf{r}, \mathbf{p})) \tag{3.13}$$

Noting that the Hamiltonian depends on beam distribution, one has to solve the implicit equation:

$$f(\mathbf{r}, \mathbf{p}) = f(H(\mathbf{r}, \mathbf{p}, f(\mathbf{r}, \mathbf{p}))) \tag{3.14}$$

Let's consider a continuous beam with cylindrical symmetry in a continuous linear focusing channel with purely radial motion. Working in (r, r') phase-space with s as an independent variable:

$$\begin{cases} \dfrac{dr}{ds} = r' = \dfrac{\partial H(r, r', s)}{\partial r'} \\ \dfrac{dr'}{ds} = -k_0^2 \cdot r + F_{\mathrm{SC}}(r, s) = -\dfrac{\partial H(r, r', s)}{\partial r} \end{cases} \tag{3.15}$$

With Hamiltonian:

$$H(r, r', s) = \frac{1}{2} \cdot r'^2 + \frac{1}{2} \cdot k_0^2 \cdot r^2 + V_{\mathrm{SC}}(r, s) \tag{3.16}$$

and V_{SC} the potential associated to the space-charge force[5]:

$$F_{\mathrm{SC}}(r, s) = -\frac{\partial V_{\mathrm{SC}}(r, s)}{\partial r}$$

Whatever the expression of $f(H)$, one has (illustrated by Figure 3.4):

- When beam is emittance dominated (hot beam):
  - The radial profile of perfectly matched beam strongly depends on f,
  - Particle trajectories in phase-space are ellipses.
- When beam is space-charge dominated (cold beam):
  - The radial profile of perfectly matched beam tends to uniform,
  - Particle trajectories in phase-space tends to rectangles.

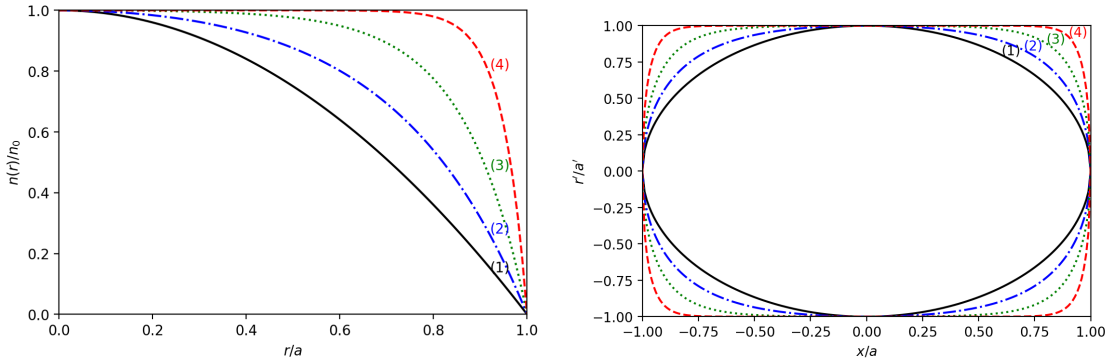

Figure 3.4: Radial density (left) and particle trajectories (right) of a beam with increasing space-charge (from 1 to 4).

On an infinite time, the beam distribution of an initially mismatched beam will match it-self as fast as the space-charge force is high.

Let's remind (seen in longitudinal and transverse beam dynamics lectures) that the **rms matching** of a beam to a focusing channel consists in adjusting beam rms parameters at channel entrance with linear (quadrupoles, bunchers) elements in order to make them:

- constant in a continuous focusing channel,
- periodic in a periodic focusing channel (same period),

Rms matching is a necessary, but not sufficient, condition to perfect matching. It is the best thing to do with linear elements to minimize emittance growth.

[5]This is not exactly a classical force in Newton, but a quantity proportional to it playing its role.

3.4 Rms-mismatch effects

When the beam is rms-mismatched, 2 phenomena contribute to **rms emittance growth** :

- The beam filamentation because space-charge is non-linear.
- **Resonant interaction** between intrinsic particle oscillation and space-charge force oscillation induced by beam envelope oscillation.

Filamentation has been explored in longitudinal beam dynamics because the longitudinal force is intrinsically non-linear. Let's explore in the following the resonant interactions between particles and beam envelope.

3.4.1 Mismatch modes

Let's use the transverse envelope equations of continuous beam to explore the effect of mismatching on the beam envelope collective motion.

Let's first assume that focusing is the same and uncoupled between x and y directions and use the horizontal envelope equation (2.43).

$$\tilde{x}'' + k_{x,0}^2(s) \cdot \tilde{x} - \frac{K}{4\tilde{x}} - \frac{\tilde{\epsilon}_x^2}{\tilde{x}^3} = 0 \tag{3.17}$$

Let $\tilde{x}_a$ be the matched beam rms size, one writes:

$$\tilde{x} = \tilde{x}_a \left(1 + \delta\right) \tag{3.18}$$

with $\delta \ll 1$ (slightly mismatched beam).

Equation (3.17) becomes at first order in δ:

$$\delta'' + \left(k_{x,0}^2(s) + \frac{K}{4 \cdot \tilde{x}_a^2} + 3\frac{\tilde{\epsilon}_x^2}{\tilde{x}_a^4} \right) \cdot \delta = 0 \tag{3.19}$$

of which the solution is:

$$\delta(s) = M \cdot \cos\left(k_{m,r} s + \varphi\right) \tag{3.20}$$

with $k_{m,r}$ the radial mismatched mode:

$$k_{m,r} = \sqrt{k_{x,0}^2(s) + \frac{K}{4 \cdot \tilde{x}_a^2} + 3\frac{\tilde{\epsilon}_x^2}{\tilde{x}_a^4}} = k_{x,0}\sqrt{2 \cdot (1 + \tilde{\eta}_x^2)} \tag{3.21}$$

The beam envelope oscillates with a spatial frequency (wave number) given by Eq. (3.21).

Particles oscillate with a phase advance per meter varying from $\eta_{x,c} \cdot k_{x,0} < \tilde{\eta}_x \cdot k_{x,0}$ (particles oscillating with small amplitude) and $k_{x,0}$ (with very large amplitude). It can

be shown that, whatever the space-charge, there is always an amplitude for which the frequency of the particle intrinsic oscillation is half the one of the radial mismatched mode:

$$\eta_{x,c} < \tilde{\eta}_x < \frac{\sqrt{2\left(1+\tilde{\eta}_x^2\right)}}{2} < 1 \tag{3.22}$$

Particle oscillation around mismatched beam, given by: $x'' + k_0(x,s)^2 \cdot x = 0$ can be written:

$$x'' + k_0(x)^2 \cdot \left(1 + \delta_k \cdot \cos\left(k_{m,r} \cdot s + \phi\right)\right) \cdot x = 0 \tag{3.23}$$

This equation, known as the **Mathieu equation** when k_0 is a constant, has been widely studied in mathematics. When $k_{m,r}$ is a multiple of k_0, the motion is unstable and the oscillation amplitude grows exponentially (order $n = \frac{k_{m,r}}{k_0}$ resonance). In our case, because k_0 depends on x, the effect is limited in amplitude.

Let's study what happens in a continuous beam without cylindrical symmetry. Equation (2.43) gives the envelope equations:

$$\begin{cases} \tilde{x}'' + k_{x,0}^2(s) \cdot \tilde{x} - \dfrac{K/2}{\tilde{x}+\tilde{y}} - \dfrac{\tilde{\epsilon}_x^2}{\tilde{x}^3} = 0 \\ \tilde{y}'' + k_{y,0}^2(s) \cdot \tilde{y} - \dfrac{K/2}{\tilde{x}+\tilde{y}} - \dfrac{\tilde{\epsilon}_y^2}{\tilde{y}^3} = 0 \end{cases} \tag{3.24}$$

Let $\tilde{x}_a$ and $\tilde{y}_a$ be the rms-matched beam dimensions. One writes:

$$\begin{cases} \tilde{x} = \tilde{x}_a\left(1+\delta_x\right) \\ \tilde{y} = \tilde{y}_a\left(1+\delta_y\right) \end{cases} \tag{3.25}$$

Equation (3.24) becomes at first order in δ_x and δ_x:

$$\begin{cases} \delta_x'' + \left(k_{x,0}^2(s) + \dfrac{K/2}{\left(\tilde{x}_a+\tilde{y}_a\right)^2} + 3\dfrac{\tilde{\epsilon}_x^2}{\tilde{x}_a^4}\right) \cdot \delta_x + \dfrac{K/2}{\left(\tilde{x}_a+\tilde{y}_a\right)^2} \cdot \delta_y = 0 \\ \delta_y'' + \left(k_{y,0}^2(s) + \dfrac{K/2}{\left(\tilde{x}_a+\tilde{y}_a\right)^2} + 3\dfrac{\tilde{\epsilon}_y^2}{\tilde{y}_a^4}\right) \cdot \delta_y + \dfrac{K/2}{\left(\tilde{x}_a+\tilde{y}_a\right)^2} \cdot \delta_x = 0 \end{cases} \tag{3.26}$$

Let's explore mismatched modes in a continuous focusing channel with the same average forces in x and y and a beam with the same x and y rms emittances. The beam has then the same matched sizes along x and y:

$$k_{x,0} = k_{y,0} = k_0 \qquad \tilde{\epsilon}_x = \tilde{\epsilon}_y = \tilde{\epsilon} \qquad \tilde{x}_a = \tilde{y}_a = \tilde{a} \tag{3.27}$$

Summing both equations of (3.26):

$$\left(\delta_x + \delta_y\right)'' + \left(k_0^2(s) + \frac{K}{4\tilde{a}^2} + 3\frac{\tilde{\epsilon^2}}{\tilde{a}^4}\right) \cdot \left(\delta_x + \delta_y\right) = 0 \tag{3.28}$$

The solution is:

$$(\delta_x + \delta_y)(s) = M \cdot \cos\left(k_{m,1} s + \varphi\right) \tag{3.29}$$

with $k_{m,1}$ the mismatch breathing mode:

$$k_{m,1} = \sqrt{k_0^2(s) + \frac{K}{4 \cdot \tilde{a}^2} + 3\frac{\tilde{\epsilon^2}}{\tilde{a}^4}} = k_0\sqrt{2 \cdot (1 + \tilde{\eta}^2)} \tag{3.30}$$

This is the same mode as this given by Eq. (3.21), corresponding to envelopes along x and y oscillating in phase.

Subtracting both equations of Eq. (3.26):

$$(\delta_x - \delta_y)'' + \left(k_0^2(s) + 3\frac{\tilde{\epsilon}^2}{\tilde{a}^4}\right) \cdot (\delta_x - \delta_y) = 0 \tag{3.31}$$

The solution is:

$$(\delta_x - \delta_y)(s) = M \cdot \cos\left(k_{m,2} s + \varphi\right) \tag{3.32}$$

with $k_{m,2}$ the mismatch quadrupole mode:

$$k_{m,2} = \sqrt{k_0^2(s) + 3\frac{\tilde{\epsilon}^2}{\tilde{a}^4}} = k_0\sqrt{1 + 3 \cdot \tilde{\eta}^2} \tag{3.33}$$

This mode corresponds to envelopes along x and y oscillating in phase opposition.

As in 1D, there are still amplitudes for which resonance of order 2 can be excited for each of the mismatch modes:

$$\eta_c < \tilde{\eta} < \frac{\sqrt{1 + 3 \cdot \tilde{\eta}^2}}{2} < 1 \tag{3.34}$$

The ratio between particle intrinsic oscillation frequencies and each of the mismatched mode frequencies are plotted in Figure 3.5, as a function of the rms space-charge tune depression. Continuous lines correspond to particles with very high amplitudes and dashed lines correspond to particles in the core. There are always amplitudes for which resonance of order 2 is excited for one of both modes. Order 3 resonance (with breathing mode) can be excited only for $\tilde{\eta} \leq 0.6$.

When the beam is bunched, 3 envelope equations result in 3 mismatched modes. Their calculation is too complex for this lecture.

3.4.2 Parametric resonances

The parametric resonance mechanism (with the external focusing) is well known in circular accelerators where it has a great impact on the choice of the working point. When the

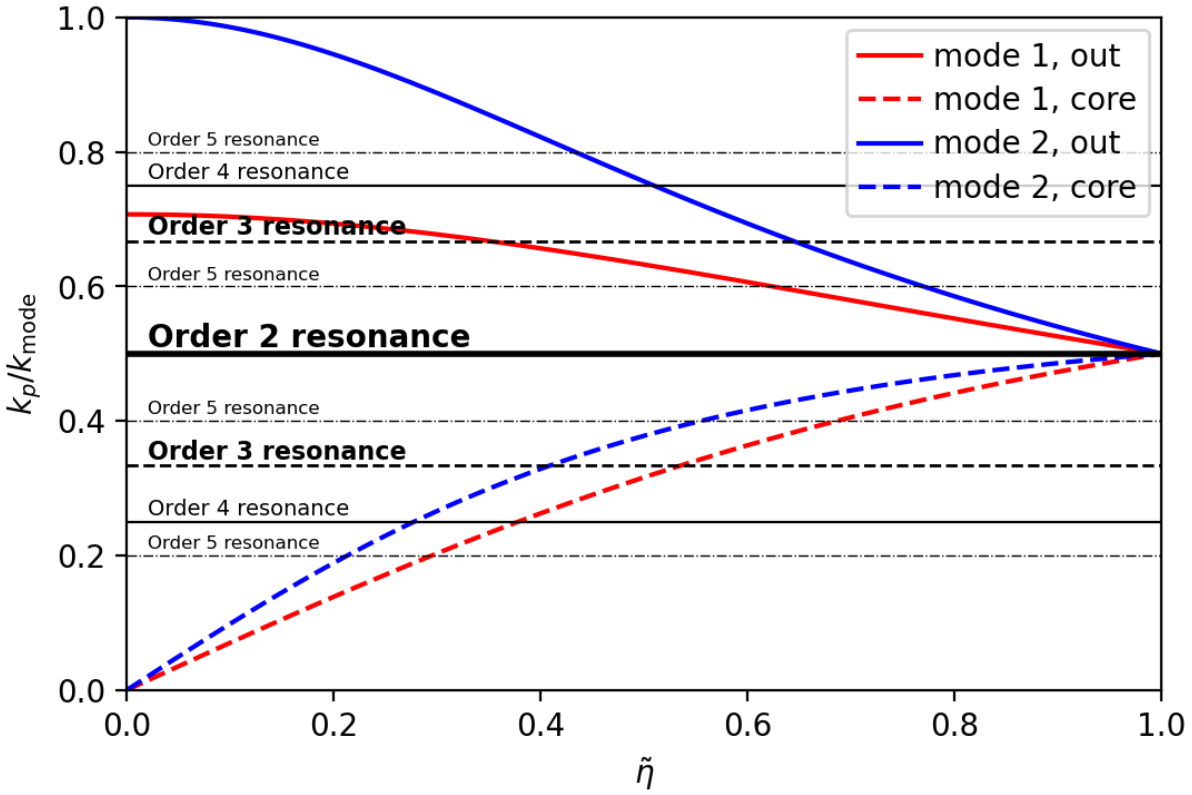

Figure 3.5: Ratio between particle intrinsic oscillation frequencies and both mismatched mode frequencies as a function of the rms space-charge tune depression. Continuous lines correspond to particles with very high amplitudes and dashed lines correspond to particles in the core.

fractional part of the wave number[6] Q is a fractional number like m/n, particles can have resonant interaction with multipole components of some accelerator elements[7]. The resonance order is n.

For example, let's consider a default in a dipole (Figure 3.6). If the field is not strong enough, particles are less deflected as they should be with an extra $\delta x'$ at each turn.

- For an integer wave number, particles come back at each turn with (about) the same horizontal oscillation phase in the dipole and extra $\delta x'$ accumulates at each turn: particle amplitude is growing.
- For a half-integer wave number, particles comes back at each turn with (about) the opposite horizontal oscillation phase in the dipole and extra $\delta x'$ compensates at each turn: particle amplitude is stable.

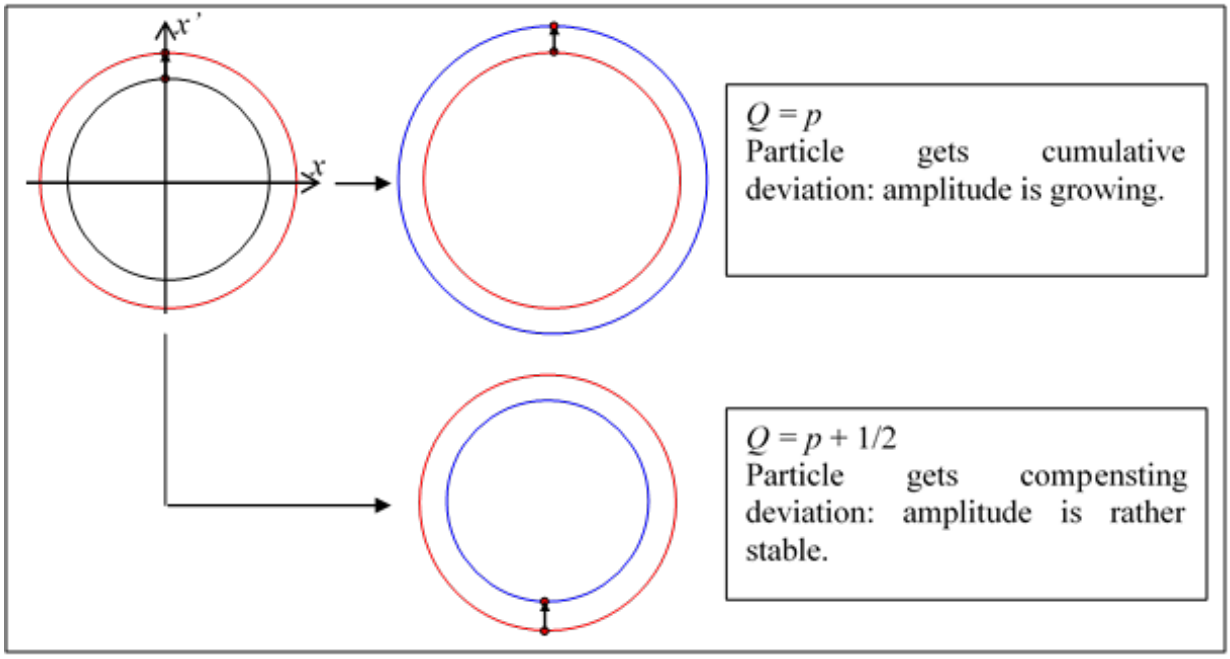

Figure 3.6: Dipole error resonance effect

If the wave number is not exactly an integer: $Q = p + \epsilon$, after $\frac{1}{2\epsilon}$ turns, the particle oscillation phase has changed by π. The particle amplitude variation is reversed. An amplitude modulation with periodicity of $1/\epsilon$ turns is observed and the longer it lasts (lower ϵ) the higher the amplitude modulation is. In Figure 3.7 the evolution of the oscillation amplitude of particle is plotted; the initial position in phase-space is $(x = 0; x' = 1)$, the extra kick is $\delta x' = 0.01$ and the wave number is $Q = 1.005$.

[6]In a circular accelerator, the wave number is the number of particle oscillations (betatron in transverse and synchrotron in longitudinal directions) in one turn.

[7]We reduce here the example in "1D", with coupling between directions.

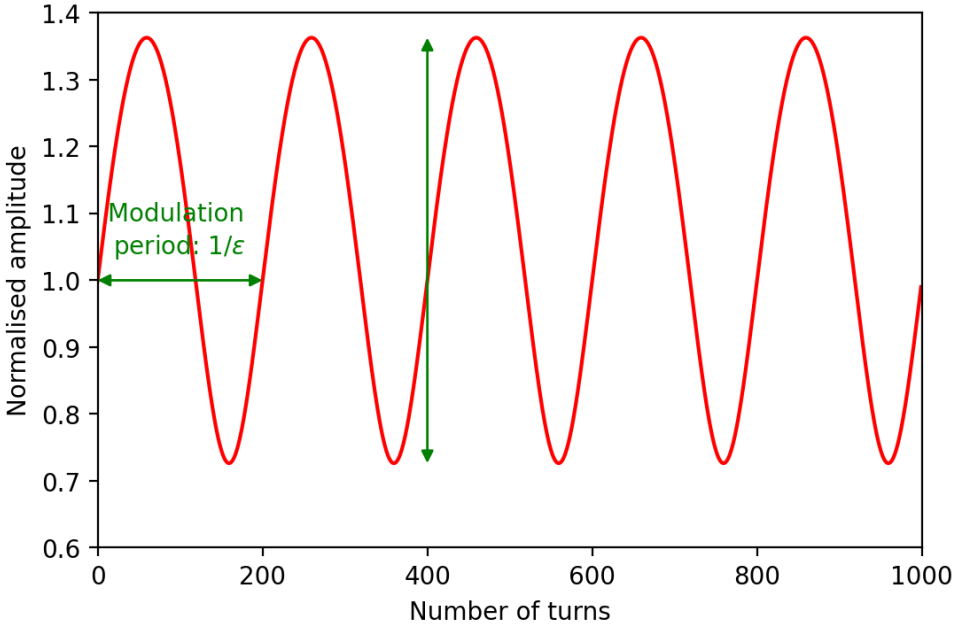

Figure 3.7: Particle amplitude modulation due to a dipole error.

The maximum particle amplitude modulation as a function of Q fractional part with initial position of the particle at $(x = 0; x' = 1)$ and an extra dipole kick of $\delta x' = 0.01$ is plotted in Figure 3.8. The closer Q from an integer, the higher the amplitude modulation is. It is given below (you can make the demonstration as an exercise) with: $k_x = 2\pi Q_x$:

$$\max \sqrt{k_x^2 \left(x(s, \delta x') - x(s, \delta x' = 0)\right)^2 + \left(x'(s, \delta x') - x'(s, \delta x' = 0)\right)^2} = \frac{\delta x'}{\sin \frac{k_x}{2}} \tag{3.35}$$

In these conditions, the chosen wave numbers (horizontal, vertical and longitudinal) are selecting (or avoiding) the potential resonances that can affect the particle motion (if associated errors exist).

Unfortunately, space-charge order 2 resonances (at least) with beam mismatched modes are always excited. Some beam particles might have amplitudes allowing an oscillation frequency being half the mismatched mode frequency (and then the force applied to the beam through space-charge force). The consequence is a modulation (increase or decrease) of the oscillation amplitude of these particles of which some could reach the beam pipe. Fortunately, since space-charge force is non-linear, amplitude change leads also to oscillation frequency change and thus a phase change compensating the effect (Figure 3.9). Moreover, Figure 3.5 shows that particles with high amplitude are far from this resonance and the effect is "limited" to a few times the beam size.

Out of the scope of this lecture, you might know that, unfortunately, in bunched beams, the resonance of order 2 can be excited to infinite amplitudes!

As the excitation of order 2 resonance is unavoidable, the best is to keep the beam

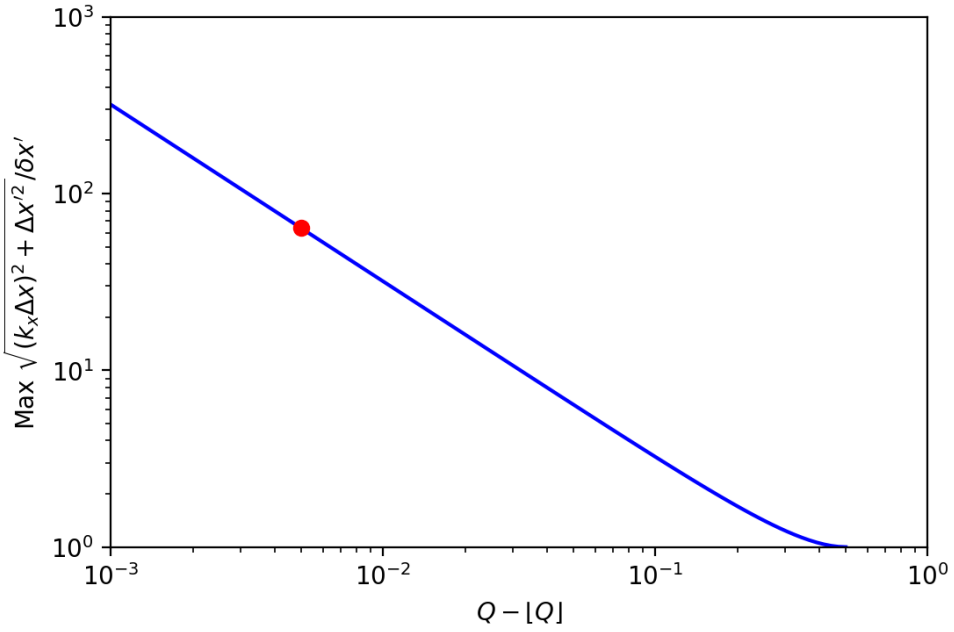

Figure 3.8: Maximal particle amplitude modulation as a function of Q fractional part.

matched to limit the emittance growth and associated halo production.

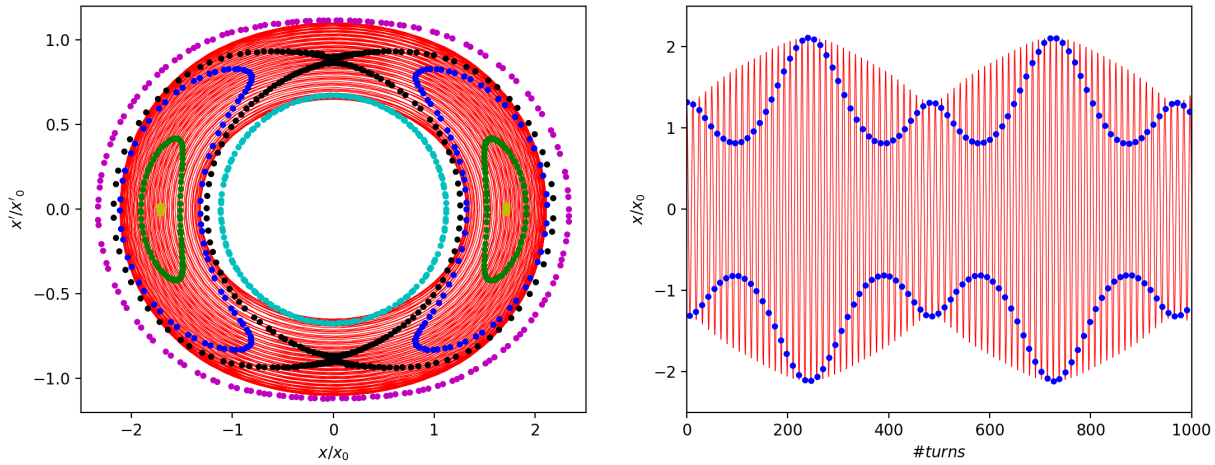

Figure 3.9: Trajectory in phase-space (left) and real space (right) of a particle feeling resonance of order 2. In red, the particle continuous trajectories. In blue, the particle positions plotted periodically with the mode period. In black and in green, the stroboscopic positions of the particles with a different initial position are shown. For small (in cyan) or large (in magenta) initial amplitudes, the trajectory is not perturbed by the mismatching resonance.

4 Wall effects

4.1 Incoherent and incoherent motion

The beam consists of many particles, each of which moves inside the beam with its individual betatron amplitude, phase, and even tune Q (under the influence of direct space charge). The **incoherent motion** describes the motion of each of these particles around the reference axis. Amplitude and phase are randomly distributed. The beam and its centre of gravity – and thus the source of the direct space-charge field – do not move (static beam).

A static beam is given a transverse fast deflection (less than 1 turn) and starts performing betatron oscillations as a whole. The **coherent motion** describes the motion of the center of mass of the beam. This is readily observed by a position monitor. Note that the source of the direct space charge is now moving: individual particles still continue their incoherent motion around the common coherent trajectory and still experience their incoherent tune shifts as well. Note the difference between the coherent and incoherent motions: the incoherent motion is for the particle around the center of mass and the coherent motion the motion of the center of mass itself.

4.2 Example of an incoherent motion: the plate conductor

4.2.1 Calculation of the resultant electric field

We have seen in Figure 1.2 that the real charge q attracts charges in the plate conductor (at a distance d). This charge distribution sets a constant potential in the conductor. It can be modelled by an image charge $-q$ symmetric of the real charge with respect to the plate.

If we consider a rectangular beam screen with the width $2w$ great compared to the height $2h$, the beam screen can be modelled as two parallel plates (see Figure 4.1). We assume a linear distribution. The electric field generated by a linear distribution λ is:

$$\mathbf{E}_\lambda(\mathbf{r}) = \frac{\lambda}{2\pi\epsilon_0}\frac{x\mathbf{e}_x + y\mathbf{e}_y}{x^2+y^2} \tag{4.1}$$

The sum of the image charges is then ($y \ll h$) and by using $\sum_{n=1}^{\infty} \frac{(-1)^n}{n^2} = -\frac{\pi^2}{12}$:

$$\mathbf{E}(x,y) = \sum_{n=1}^{\infty} \frac{(-1)^n \lambda}{2\pi\epsilon_0} \left[\frac{x\mathbf{e}_x + (2nh-y)\mathbf{e}_y}{x^2+(2nh-y)^2} + \frac{x\mathbf{e}_x - (2nh+y)\mathbf{e}_y}{x^2+(2nh+y)^2} \right] \tag{4.2}$$

$$\approx \frac{\lambda}{\pi\epsilon_0} \sum_{n=1}^{\infty} (-1)^n \left[\frac{x\mathbf{e}_x - y\mathbf{e}_y}{4n^2h^2} + o(x,y) \right] \tag{4.3}$$

$$\approx \frac{I}{\beta c \pi \epsilon_0} \frac{\pi^2}{48h^2} \left(-x\mathbf{e}_x + y\mathbf{e}_y + o(x,y) \right) \tag{4.4}$$

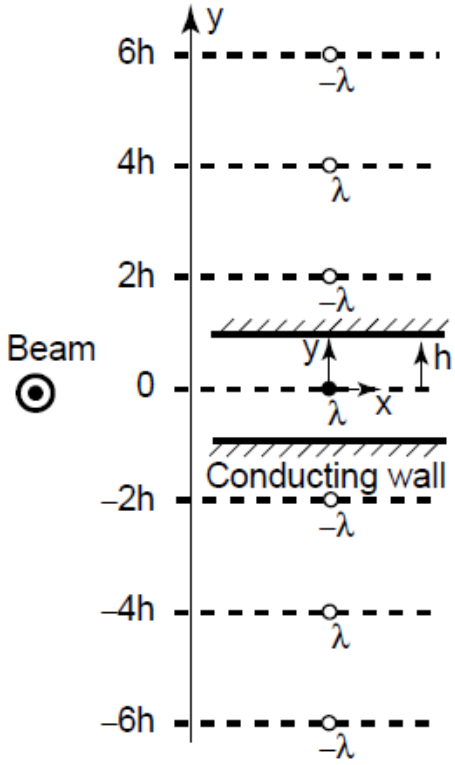

Figure 4.1: Series of the image charges generated by two parallel plates

4.2.2 Tune shift if beam between two plates

If we consider a uniform elliptical continuous beam, the motion equations become:

$$\begin{cases} \dfrac{dx'}{ds} = -k_{x,0}^2 \cdot x + F'_{x,\mathrm{SC}}(\mathbf{r}, s) = -k_{x,0}^2 \cdot x + \dfrac{F_{x,\mathrm{SC}}(\mathbf{r}, s)}{\gamma\beta^2 m_0 c^2} \\ \dfrac{dy'}{ds} = -k_{y,0}^2 \cdot y + F'_{y,\mathrm{SC}}(\mathbf{r}, s) = -k_{y,0}^2 \cdot y + \dfrac{F_{y,\mathrm{SC}}(\mathbf{r}, s)}{\gamma\beta^2 m_0 c^2} \end{cases} \tag{4.5}$$

$$\begin{cases} \dfrac{dx'}{ds} + \left[k_{x,0}^2 - \dfrac{q}{\pi\epsilon_0 m_0 c^3} \dfrac{I}{\beta^3\gamma} \left(\dfrac{1}{\gamma^2 X \cdot (X+Y)} - \dfrac{\pi^2}{48h^2} \right) \right] \cdot x = 0 \\ \dfrac{dy'}{ds} + \left[k_{y,0}^2 - \dfrac{q}{\pi\epsilon_0 m_0 c^3} \dfrac{I}{\beta^3\gamma} \left(\dfrac{1}{\gamma^2 Y \cdot (X+Y)} + \dfrac{\pi^2}{48h^2} \right) \right] \cdot y = 0 \end{cases} \tag{4.6}$$

$$\begin{cases} k_{x,\mathrm{inc}} = \eta_x k_{x,0} = k_{x,0} \left[1 - \dfrac{q}{\pi\epsilon_0 m_0 c^3} \dfrac{I}{\beta^3\gamma k_{x,0}^2} \left(\dfrac{1}{\gamma^2 X \cdot (X+Y)} - \dfrac{\pi^2}{48h^2} \right) \right]^{1/2} \\ k_{y,\mathrm{inc}} = \eta_y k_{y,0} = k_{y,0} \left[1 - \dfrac{q}{\pi\epsilon_0 m_0 c^3} \dfrac{I}{\beta^3\gamma k_{y,0}^2} \left(\dfrac{1}{\gamma^2 Y \cdot (X+Y)} + \dfrac{\pi^2}{48h^2} \right) \right]^{1/2} \end{cases} \tag{4.7}$$

4.2.3 Wall effects against direct space-charge

- The electric image field is vertically defocusing, but horizontally focusing (sign of image term changes), which by the way is not just a feature of this particular geometry, but is typical for most synchrotrons with their rather flattish vacuum pipes;
- The field is larger for small chamber height h;
- Image effects decrease with $1/\gamma$, much slower than the direct space-charge term $(1/\gamma^3)$, and thus are of some concern for electron and high-energy proton machines.
- The incoherent motion can be measured by using a quadrupole lens and by introducing a mismatching. The envelope oscillation period gives the incoherent tune by dividing by 2.

4.3 Example of a coherent motion: Circular conductor

4.3.1 Calculation of the electric field of a beam offset in a circular pipe

We have seen in Figure 1.3 that The charge distribution on a cylindrical conductor of radius R by a linar charge per meter λ at a distance a from the cylinder center can be modelled by a charge per linear meter $-\lambda$ on the charge-cylinder center axis at distance b such as $a \cdot b = R^2$. The field is equivalent to the one generated by a linear charge $-\lambda$ at the position $x = R^2/a$.

Let us consider a linear distribution with an offset of $\mathbf{r_0} = x_0\mathbf{e}_x + y_0\mathbf{e}_y$. The equivalent charge image of the beam pipe is a linear distribution $-\lambda$ at the position $\mathbf{r_1} = \frac{R^2}{r_0^2}\mathbf{r_0}$. The electric field at the beam center is then:

$$\mathbf{E}_\lambda(\mathbf{r_0}) = \frac{\lambda}{2\pi\epsilon_0}\frac{\mathbf{r_1}-\mathbf{r_0}}{\|\mathbf{r_1}-\mathbf{r_0}\|^2} = \frac{\lambda}{2\pi\epsilon_0}\frac{\mathbf{r_0}}{R^2-r_0^2} = \frac{\lambda}{2\pi\epsilon_0}\frac{\mathbf{r_0}}{R^2} + o(x_0, y_0) \tag{4.8}$$

The motion equations and tune shift become:

$$\begin{cases} \dfrac{dx_0'}{ds} = -k_{x,0}^2 \cdot x_0 + \dfrac{F_{x,\mathrm{SC}}(\mathbf{r}, s)}{\gamma\beta^2 m_0 c^2} = \left[-k_{x,0}^2 + \dfrac{q}{\pi\epsilon_0 m_0 c^3}\dfrac{I}{\beta^3\gamma}\dfrac{1}{2R^2}\right]\cdot x_0 \\ \dfrac{dy_0'}{ds} = -k_{y,0}^2 \cdot y_0 + \dfrac{F_{y,\mathrm{SC}}(\mathbf{r}, s)}{\gamma\beta^2 m_0 c^2} = \left[-k_{y,0}^2 + \dfrac{q}{\pi\epsilon_0 m_0 c^3}\dfrac{I}{\beta^3\gamma}\dfrac{1}{2R^2}\right]\cdot y_0 \end{cases} \tag{4.9}$$

$$\begin{cases} k_{x,\mathrm{coh}} = \eta_x k_{x,0} = k_{x,0}\left[1 - \dfrac{q}{\pi\epsilon_0 m_0 c^3}\dfrac{I}{\beta^3\gamma k_{x,0}^2}\dfrac{1}{2R^2}\right]^{1/2} \\ k_{y,\mathrm{coh}} = \eta_y k_{y,0} = k_{y,0}\left[1 - \dfrac{q}{\pi\epsilon_0 m_0 c^3}\dfrac{I}{\beta^3\gamma k_{y,0}^2}\dfrac{1}{2R^2}\right]^{1/2} \end{cases} \tag{4.10}$$

4.3.2 A few features of the coherent tune shift

- The force is linear in $\bar{\mathbf{r}}$, so there is a coherent tune shift.
- The $1/\gamma$ dependence of the tune shift comes from the fact that the charged particles induce the electrostatic field and thus generate a force proportional to their number, but independent of their mass, whereas the deflection of the beam by this force is inversely proportional to their mass $m_0\gamma$.
- The coherent tune shift is never positive.
- Note that a perfectly conducting beam pipe has been assumed here, for simplicity. The effects of a thin vacuum chamber with finite conductivity are more subtle.
- The coherent tune shift can be measured by deflecting the beam with a transverse kicker (with a gate shorter than one revolution period) and by measuring the position (in a ring, turn after turn or in a linac at different positions) with a beam position monitor.

5 Conclusion – *To the lecture frontiers*

In this lecture, we explore the calculation of space-charge force and analyse its effects on beam dynamics in an accelerator. This conclusion summarizes, without specific pedagogic care, main encountered mechanisms. Paragraphs in italic address the frontier of this exciting discipline where many things are still to be discovered, formulated and communicated to the beam physicist community.

The space-charge electromagnetic force is made of a centrifugal electric component (from beam center) and a centripetal magnetic force. In vacuum, magnetic component tends to compensate the electric one when the beam energy (γ) tends to infinity even if it can never totally cancel it. It generally consists in dividing the electric force by γ^2.

This reduction in $1/\gamma^2$ is a very popular assumption, true only in a perfectly parallel monochromatic beam. In other cases, it can lead to significant underestimation of the space-charge force. A better expression of the magnetic force can be given by (1.23)*. For example, considering a beam with $\gamma \gg 1$ focused with an angle $x' \ll 1$. A first estimation of the error of the model in $1/\gamma^2$ is about: $(\gamma \cdot x')^2$. It is moreover radial dependent. This may have non negligible consequences in the final focusing line in a very high energy collider where the beam is strongly focused.*

At low energy, space-charge effects are strong and can limit the available beam intensity. They can be compensated by adding other charges in the beam neighbourhood. For example, in the accelerator pipe, beam gradually ionizes atoms of the residual gas producing positive ions and electrons. Charges, opposite to beam charge, can be partially trapped in the beam potential well reducing dynamically the electric field and then the space-charge force. After a transient time, equilibrium in which space-charge force is reduced (even reversed) is reached. The transit time and the final equilibrium depend essentially on: the beam intensity, its time structure, the vacuum chamber geometry, the gas composition and pressure and differential cross sections of ionization, capture and heat exchange. Some trapped particle can gain energy along the accelerator reducing the magnetic force.

The analytic expression of space-charge field can be obtained for some charge and current distributions. Nevertheless, in most actual cases, it has to be calculated numerically with specific algorithms. In general, the computation is made in beam frame (using Lorentz transform) where particles are non-relativistic and the magnetic force is negligible with respect to the electric one. The most efficient routines spread the beam charge on mesh where the field is calculated. New particle coordinates are obtained in laboratory frame. These algorithms induce perturbations which have to be carefully managed.

When the beam is strongly accelerated (like in electron guns), it is essential to cope with the retarded electromagnetic field (Lienard-Wiechert) or to solve field transport equations (Maxwell) at the same time as the particles. In the same way, when the beam is ultra-

relativistic, synchrotron radiation in magnet cannot be neglected and the particle can also be relativistic in the beam frame. Typically, be cautious to the limits of the space-charge routines you use and verify that the model it uses is compatible to simulated situation.

Some space-charge routines cope with the beam environment. Usually, they do it in static approximation (image charge) without taking into account induced charge displacement in the specific vacuum chamber geometry.

Vacuum chamber specific geometries can contribute to extra-field production (stationary, transient or oscillating) of which the effects on beam dynamics have to be taken into account. These fields can be modelled by modes or impedances (complex, frequency dependent) modelling the spatial configuration and time evolution of field amplitude as a function of beam spatial or time structures.

In first approximation, the beam can be modelled by a 6×6 sigma matrix being the variance-covariance of the beam distribution. The transport of this matrix is made with particle transfer matrix of accelerator elements (linear or linearised). The space-charge force can be linearised from a specific integration over the particle distribution which is equivalent to the space-charge force in an equivalent (with the same sigma matrix) uniform distribution. The space-charge force can then by modelled by a matrix which has been applied frequently because its coefficients depend on beam dimensions. This linear model is valid while the beam rms emittance is (almost) constant.

Unfortunately, the space-charge force is intrinsically non-linear, which induces emittance growth, especially if the beam is mismatched in the accelerator. The "matching" concept is especially valid in periodic structures which can be modelled by a continuous focusing channel (with permanent focusing force) where a perfectly matched beam has a stationary distribution (on which phase-space density is constant over curves on which motion Hamiltonian is constant). With conventional (linear) transport elements a real beam can only be, at the best, rms matched to the structure. It consists in making the evolution of the sigma matrix (pseudo-)periodic (with the same period of the structure). This rms-matching is a necessary but not sufficient condition for perfect matching.

When the beam is not perfectly matched, its phase-space distribution is going gradually (with emittance growth) to homogenize on particle trajectories until being completely perfectly matched. If the beam is rms matched, this emittance growth is limited (as much as possible).

One should note that phase-space volume occupied by beam particles is never modified: it is strictly zero if particles are considered as perfect dots or very low if they are considered as quantic fermions of which the dimension is given by Heisenberg's uncertainty principle ($\delta x \cdot \delta p \approx \hbar = 1.054 \times 10^{-34}\,\mathrm{kg\,m\,s^{-2}}$, *giving a normalised phase-space sub-volume of* $\delta V = \left(\frac{\delta x \cdot \delta p \cdot c}{mc^2}\right)^3 = (2.1 \times 10^{-10}\,\mu\mathrm{m})^3$ *for protons or* $\delta V = (3.9 \times 10^{-7}\,\mu\mathrm{m})^3$ *for electrons, which is far from what is actually achieved in accelerator (*$1\,\mathrm{nC}$ *;* $1\pi\,\mu\mathrm{m}$*). If one considers that the beam is a continuum phase-space density of which the evolution is given by Vlasov equation, this conservation is called the Liouville theorem.*

The rms emittance is a statistical beam size in phase-space. Its growth (through filamentation in particular) says that phase-space distribution is mixed and it may be very

difficult to "un-mix" it (revert the mixing).

Nevertheless, rms-emittance growth may be followed by reduction in non-linear varying forces. It is similar to a red blob of paint in a yellow paint pot. The more you mix the paint, the more it is difficult (unlikely) to recover the red paint by turning in the reverse.

If the beam is not perfectly matched, its distribution evolves toward an equilibrium and particle feels a varying space-charge force during its (betatron or synchrotron) oscillation motion. Besides filamentation and stochastic variations, some particles can feel resonant interaction with the space-charge force if their intrinsic oscillation period is a multiple of the beam sizes oscillation. When the beam is initially rms-mismatched, its average size (envelope) oscillates in a superposition of 3 mismatch-modes (or less (degenerated) in specific geometries). The resonant particles can gain (or lose) amplitude alternatively. It exists amplitudes for which the resonance of order 2 with mismatch-mode is always excited. Because beam density is usually radial decreasing, there are more particle gaining amplitude than losing amplitude leading to emittance growth and halo formation. As in the same time, beam matches itself to the transport channel, many particles will conserve the gained amplitude.

A linear accelerator is made of many different structures chosen for their acceleration efficiencies as a function of the beam energy. Generally, each structure applies a pseudo- periodic focusing (longitudinal or transverse) to the beam. In these conditions, a rms-matched beam envelope has the same pseudo-period as the external force. Between structures, a section dedicated to the rms-matching to the next structure is necessary (the upstream or/and downstream structures can play this role). One needs at least 1 adjustable element per phase-space independent direction, usually 4 (mainly) transverse and 2 (mainly) longitudinal.

6 Annex

6.1 Annex 1: dimensions

The equation analysis using the quantities dimensions (units) help "feeling" the physics, and, sometimes, verifying their pertinence. Here are the dimensions of all quantities used in the lecture, their relation with basic dimensions[1] and origin equations.

Quantity	Usual dimension	Symbol dimension	Basis dimension	Origin equation
Distance (l)	meter	$[\mathrm{m}]$	$[\mathrm{m}]$	
Time (s)	second	$[\mathrm{s}]$	$[\mathrm{s}]$	
Velocity (v)		$[\mathrm{m\,s^{-1}}]$	$[\mathrm{m\,s^{-1}}]$	$v = \frac{dl}{dt}$
Acceleration (a)		$[\mathrm{m\,s^{-2}}]$	$[\mathrm{m\,s^{-2}}]$	$a = \frac{dv}{dt}$
Mass (m)	kilogram	$[\mathrm{kg}]$	$[\mathrm{kg}]$	
Force (F)	Newton	$[\mathrm{N}]$	$[\mathrm{kg\,m\,s^{-2}}]$	$F = m \cdot a$
Energy (W)	Joule	$[\mathrm{J}]$	$[\mathrm{kg\,m^2\,s^{-2}}]$	$W = F \cdot l$
Power (P)	Watt	$[\mathrm{W}]$	$[\mathrm{kg\,m^2\,s^{-3}}]$	$P = \frac{dW}{dt}$
Electric charge (q)	Coulomb	$[\mathrm{C}]$	$[\mathrm{C}]$	
Electric current (I)	Ampere	$[\mathrm{A}]$	$[\mathrm{C\,s^{-1}}]$	$I = \frac{dq}{dt}$
Electric field (E)	Volt per meter	$[\mathrm{V\,m^{-1}}]$	$[\mathrm{kg\,m\,s^{-2}\,C^{-1}}]$	$F = q \cdot E$
Potential (U)	Volt	$[\mathrm{V}]$	$[\mathrm{kg\,m^2\,s^{-2}\,C^{-1}}]$	$E = -\frac{dU}{dl}$
Magnetic field (B)	Tesla	$[\mathrm{T}]$	$[\mathrm{kg\,s^{-1}\,C^{-1}}]$	$F = q \cdot v \cdot B$
Magnetic vector potential (A)	Tesla.meter	$[\mathrm{T\,m}]$	$[\mathrm{kg\,m\,s^{-1}\,C^{-1}}]$	$\mathbf{B} = \nabla \times \mathbf{A}$
Resistance (R)	Ohm	$[\Omega]$	$[\mathrm{kg\,m^2\,s^{-1}\,C^{-2}}]$	$U = R \cdot I$
Capacity (C)	Farad	$[\mathrm{F}]$	$[\mathrm{C^2\,s^2\,kg^{-1}\,m^{-2}}]$	$q = C \cdot U$
Inductance (L)	Henry	$[\mathrm{H}]$	$[\mathrm{kg\,m^2\,C^{-2}}]$	$U = -L \cdot \frac{dI}{dt}$
Charge density (ρ)		$[\mathrm{C\,m^{-3}}]$	$[\mathrm{C\,m^{-3}}]$	$dq = \rho \cdot dl^3$
Current density (j)		$[\mathrm{A\,m^{-2}}]$	$[\mathrm{C\,s^{-1}\,m^{-2}}]$	$dI = j \cdot dl^2$

[1] Many basis are possible. International System has been used but Ampere has been replaced by Coulomb, which seems more "physical".

6.2 Annex 2: Lorentz transforms

In electromagnetic calculation, it is usual to change frame in order to cancel magnetic component of electromagnetic field (beam frame). If $\mathcal{R}'$ is a moving frame with reduced velocity $\beta = \beta \cdot \mathbf{e}_z$ in frame $\mathcal{R}$.

Relationships between time t and spatial coordinates (x, y, z) expressed in both frames (with or without prime) are given by:

$$\begin{cases} ct = \gamma \cdot (ct' + \beta \cdot z') \\ x = x' \\ y = y' \\ z = \gamma \cdot (z' + \beta \cdot ct') \end{cases} \iff \begin{cases} ct' = \gamma \cdot (ct - \beta \cdot z) \\ x' = x \\ y' = y \\ z' = \gamma \cdot (z - \beta \cdot ct) \end{cases} \tag{6.1}$$

with γ the Lorentz factor, and c the speed of light in vacuum.

Relationships between energy W and momentum component (p_x, p_y, p_z) expressed in both frames (with or without prime) are given by:

$$\begin{cases} W = \gamma \cdot (W' + \beta \cdot p'_z) \\ p_x = p'_x \\ p_y = p'_y \\ p_z = \gamma \cdot (p'_z + \beta \cdot W') \end{cases} \iff \begin{cases} W' = \gamma \cdot (W - \beta \cdot p_z) \\ p'_x = p_x \\ p'_y = p_y \\ p'_z = \gamma \cdot (p_z - \beta \cdot W) \end{cases} \tag{6.2}$$

Relationships between electric field components (E_x, E_y, E_z) and magnetic field components (B_x, B_y, B_z) expressed in both frame (with or without prime) are given by:

$$\begin{cases} E_x = \gamma \cdot \left(E'_x + \beta \cdot cB'_y\right) \\ E_y = \gamma \cdot \left(E'_y - \beta \cdot cB'_x\right) \\ E_z = E'_z \\ cB_x = \gamma \cdot \left(cB'_x - \beta \cdot E'_y\right) \\ cB_y = \gamma \cdot \left(cB'_y + \beta \cdot E'_x\right) \\ cB_z = cB'_z \end{cases} \iff \begin{cases} E'_x = \gamma \cdot (E_x - \beta \cdot cB_y) \\ E'_y = \gamma \cdot (E_y + \beta \cdot cB_x) \\ E'_z = E_z \\ cB'_x = \gamma \cdot (cB_x + \beta \cdot E_y) \\ cB'_y = \gamma \cdot (cB_y - \beta \cdot E_x) \\ cB'_z = cB_z \end{cases} \tag{6.3}$$

Index